P.41

FEEDBACK CONTROL LAWS FOR HIGHLY MANEUVERABLE AIRCRAFT

GRANT NAG 1 - 1380

INTERIM REPORT
JANUARY - JULY 1992

PRINCIPAL INVESTIGATORS

DR. WILLIAM L. GARRARD
DR. GARY J. BALAS

GRADUATE RESEARCH ASSISTANT

JACOB REINER

DEPARTMENT OF AEROSPACE ENGINEERING AND MECHANICS
UNIVERSITY OF MINNESOTA
MINNEAPOLIS MN 55455

NASA TECHNICAL MONITOR

DR. BART BACON

LANGLEY RESEARCH CENTER

HAMPTON VA 23665

(NASA-CR-190535) FEEDBACK CONTROL LAWS FOR HIGHLY MANEUVERABLE AIRCRAFT Interim Report, Jan. - Jul. 1992 (Minnesota Univ.) 41 p

N92-29654

Unclas
G3/08 0109003

Abstract

This report presents the results of a study of the application of H_∞ and μ synthesis techniques to the design of feedback control laws for the longitudinal dynamics of the High Angle of Attack Research Vehicle (HARV). The objective of this study is to develop methods for the design of feedback control laws which cause the closed loop longitudinal dynamics of the HARV to meet handling quality specifications over the entire flight envelope. Control law designs are based on models of the HARV linearized at various flight conditions. The control laws are evaluated by both linear and nonlinear simulations of typical maneuvers. The fixed gain control laws resulting from both the H_∞ and μ synthesis techniques result in excellent performance even when the aircraft performs maneuvers in which the system states vary significantly from their equilibrium design values. Both the H_∞ and μ synthesis control laws result in performance which compares favorably with an existing baseline longitudinal control law.

1 Introduction

The overall objective of this research program is to develop control law design techniques for aircraft which operate in regimes in which nonlinearities in the equations of motion have an important effect on the dynamic response characteristics. Our long term goal is to develop a design methodology which combines nonlinear dynamic inversion and μ synthesis techniques. This should result in nonlinear control laws with performance and stability characteristics which are robust to modeling errors and parameter variations. For the initial stage of this research, we studied the application of H_∞ and μ synthesis techniques to the design of longitudinal control laws for the HARV. This report summarizes the results of this study.

The open loop longitudinal dynamics of the HARV do not meet standard aircraft handling quality requirements at low speeds and relatively high angles of attack. Our design objective is to develop control laws which result in closed loop dynamic response characteristics which meet these requirements. These control laws must not result in saturation of actuator deflection and deflection rates. The μ synthesis control laws are explicitly designed to be insensitive to (1) parameter uncertainties in the linear design models, (2) uncertainty in the effectiveness of the actuators, (3) uncertainty in the sensor measurements and (4) input uncertainties including higher order dynamics.

Our basic philosophy is to design control laws which minimize the weighted H_∞ norm of the difference between the actual aircraft pitch rate, angle of attack, and/or normal acceleration

responses to pilot stick inputs and the desired responses to these inputs as given by models based on standard handling quality specifications. Furthermore we wish to perform this minimization without saturating our control actuators. To achieve this goal we minimize the weighted H_∞ norm of the actuator deflection and deflection rates.

We learned two important lessons which have general applicability to H_∞ based techniques for aircraft control law design. First, we found that it was important to include phugoid dynamics in our model of desired aircraft handling qualities. H_∞ based techniques, including μ synthesis, minimize the H_∞ norm of the weighted system output over the entire frequency range. In the case of aircraft handling qualities enhancement, part of the output vector is the difference between some of the actual aircraft states and the desired values of these states as predicted by models which reflect the handling quality specifications. If there is a significant difference between the desired and actual aircraft response in a particular frequency range, H_∞ based techniques will produce control laws which act to minimize this difference. If this difference occurs in a frequency range in which we are not interested in optimizing performance, the resulting control laws may not give very good results in frequency ranges in which performance is important. Most aircraft handling quality specifications are given in terms of short period response characteristics. If we formulate these characteristics in terms of transfer functions, the low frequency characteristics will in general be different from those of the actual aircraft since the phugoid mode has been neglected. In the case of angle of attack response, the phugoid mode cancels out of the transfer function and the low frequency response from the handling quality model and the aircraft are essentially identical. This is not the case for the pitch and normal acceleration responses and the low frequency gains for the aircraft are considerably less than those of the short period handling quality models. In order to achieve good tracking of pilot inputs, it is essential to include some model of the phugoid dynamics in the handling quality models. It might be possible to achieve good tracking by suitable choice of output error weighting functions, i.e. reduced error weighting at low frequency, but the addition of a phugoid mode to the handling quality model is a natural way of addressing the problem which allows us to achieve both short period and phugoid handling quality specifications. This can be important at flight conditions at which the phugoid is lightly damped or unstable.

Second, we found that is important to add a pilot stick shaping or pre-filter following the pilot input. Otherwise the control law acts to provide performance at high frequencies at which precise tracking is not needed at the expense of performance in the low frequency range in which tracking is important.

Although the design techniques described in this report can be applied to a variety of handling

quality objectives, we concentrate on having the pitch rate follow pilot stick inputs at low angles of attack and the angle of attack follow pilot inputs at high angles of attack. H_∞ and μ synthesis control laws are designed for linearized models of the HARV at several flight conditions. These control laws are evaluated using linear and nonlinear simulations of the HARV. The nonlinear simulations include lateral dynamics and the baseline lateral control laws included in the simulation are used. Both the H_∞ and μ synthesis control laws follow pilot inputs well and meet handling quality specifications. In the linear simulations the μ synthesis control laws exhibit less sensitivity to parameter variations than do the H_∞ control laws, however, both sets of control laws exhibit almost identical responses in nonlinear simulations in which transient values of the state vary substantially from their equilibrium values. Both sets of control laws yield responses which are similar to those obtained with the baseline longitudinal control laws which were included with the simulation.

The remainder of this report is divided into six sections. The next section gives a brief overview of the H_∞ and μ design methodologies. The third section describes the handling quality models used. These are based on recent handling quality specifications [1]. The fourth section details the H_∞ design and includes a method for optimal allocation of control effort between the stabilizers and the thrust vector control (TVC). The fifth section describes the μ synthesis design. The sixth section introduces a comparison between the performance of one of our control laws and the baseline controller. The seventh section consists of conclusions and future research directions.

2 Controller Synthesis Techniques

2.1 H_∞ Controller Synthesis

In recent years there has been great interest in controller design based on H_∞ control theory [2–7]. A substantial contribution to the solution of the H_∞ problem has resulted from the state space representation of the problem [5]. The H_∞ space is a Hilbert space [8] consisting of the bounded and stable functions. The H_∞ norm of a real rational matrix T(s) is defined as:

$$\|T\|_\infty = \sup_{Re(s)>0} \|T(s)\| = \sup_{\omega} \|T(j\omega)\| = \sup_{\omega} \bar{\sigma}[T(j\omega)] \quad (1)$$

where $\bar{\sigma}[T(j\omega)]$ denotes the largest singular value of $T(j\omega)$ over frequency. Restricting the plants to Linear Time Invariant (LTI), the basic system, called P, considered in the H_∞

synthesis is described by :

$$\dot{x}(t) = A\,x(t) + B_1 w(t) + B_2 u(t) \tag{2}$$

$$z(t) = C_1 x(t) + D_{11} w(t) + D_{12} u(t) \tag{3}$$

$$y(t) = C_2 x(t) + D_{21} w(t) + D_{22} u(t) \tag{4}$$

where $x(t)$ is an n dimensional state vector, $w(t)$ is an m_1 dimensional disturbance vector, $u(t)$ is an m_2 dimensional control vector, $z(t)$ is a p_1 dimensional output vector whose magnitude is to be minimized and $y(t)$ is a p_2 dimensional measurement vector.

The objective of H_∞ control synthesis is to find a stabilizing controller K, whose input is $y(t)$ and whose output is $u(t)$, that will minimize the H_∞ norm of the transfer function between $w(t)$ and $z(t)$. When such a controller is found, the following condition is satisfied :

$$\|T_{zw}\|_\infty \leq \gamma \tag{5}$$

with γ being the least upper bound of the H_∞ norm. Solution for the H_∞ controller involves the solution of two Algebraic Ricatti Equations (A.R.E) [4,5]. The first A.R.E to be solved is related to the full information case represented by the Hamiltonian matrix I_∞. The second A.R.E is related to the output estimation case. This A.R.E is represented by the Hamiltonian matrix J_∞. The matrices I_∞ and J_∞ are given below.

$$I_\infty = \begin{bmatrix} A & \gamma^{-2} B_1 B_1' - B_2 B_2' \\ -C_1' C_1 & -A' \end{bmatrix} \tag{6}$$

$$J_\infty = \begin{bmatrix} A' & \gamma^{-2} C_1' C_1 - C_2' C_2 \\ -B_1 B_1' & -A \end{bmatrix} \tag{7}$$

The software used for controller synthesis [2] implements the bisection method on γ to find the admissible controller which simultaneously satisfies equation (5) and the following three conditions:

- $I_\infty \in dom(Ric)$ and $X_\infty = Ric(I_\infty) \geq 0$.
- $J_\infty \in dom(Ric)$ and $Y_\infty = Ric(J_\infty) \geq 0$.
- $\rho(X_\infty Y_\infty) < \gamma^2$

Where ρ stands for the spectral radius of a matrix. A matrix belongs to $dom(Ric)$ if 1) None of its eigenvalues are on the imaginary axis and 2) it has an n dimensional invariant

subspace X_H which corresponds to the n L.H.P eigenvalues which can be partitioned to $X\_H = (X_1 \quad X_2)'$ with X_1 being invertible.

In such a case, the controller is defined by the following :

$$K(s) = \left[\begin{array}{c|c} \hat{A_\infty} & -Z_\infty L_\infty \\ \hline F_\infty & 0 \end{array}\right] \tag{8}$$

where:

$$\begin{aligned} \hat{A_\infty} &= A + \gamma^{-2} B_1 B_1' X_\infty + B_2 F_\infty + Z_\infty L_\infty C_2 \\ F_\infty &= -B_2' X_\infty \\ L_\infty &= -Y_\infty C_2' \\ Z_\infty &= (I - \gamma^{-2} Y_\infty X_\infty)^{-1} \end{aligned} \tag{9}$$

In addition to the constraints given above, the system must meet the following 4 conditions:

1. (A, B_2) is stabilizable and (C_2, A) is detectable.
2. D_{12} and D_{21} have full rank.
3. $\left[\begin{array}{cc} A - j\omega I & B_2 \\ C_1 & D_{12} \end{array}\right]$ has full rank for all ω.
4. $\left[\begin{array}{cc} A - j\omega I & B_1 \\ C_2 & D_{21} \end{array}\right]$ has full rank for all ω.

The first assumption is necessary for the existence of a stabilizing controller. The second means that the penalty on z includes a nonsingular normalized penalty on the control u, w includes both plant disturbance and sensor noise, and the sensor noise weighting is normalized and nonsingular.

The third and fourth asumptions together with the first one guarantee that the two Hamiltonian matrices involved in the solution belong to $dom(Ric)$. These two assumptions are necessary for the solution described above.

The assumption of unstructured disturbances results in the H_∞ synthesis producing a controller which is usually conservative in the sense that the performance and robustness of the closed loop system are underestimated. The more realistic case of structured uncertainties is taken into consideration with μ analysis. The scaling matrices from μ analysis make it possible for the designer synthesize a less conservative controller than is obtainable from the standard H_∞ formulation. The use of μ for analysis and then for synthesis is described in detail in the following two sections.

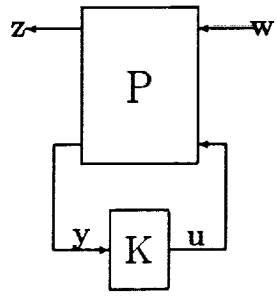

Figure 1: The Linear Fractional Transformation (LFT) $M = T_{zw} = F_l(P, K)$

2.2 μ Analysis

Let us first define μ for a given matrix $M \in C^{n \times n}$. In the definition of $\mu(M)$ there is an underlying structure $\Delta \in \mathbf{\Delta}$ where $\mathbf{\Delta}$ is a prescribed set of block diagonal matrices. We will partition $\mathbf{\Delta}$ into the following form:

$$\mathbf{\Delta} = \{diag(\delta_1 I_{r1}, ..., \delta_s I_{rs}, \Delta_1, ..., \Delta_F) : \delta_i \in C, \Delta_j \in C^{m_j \times m_j}\} \tag{10}$$

where r stands for the repeated scalar blocks, Δ for a full matrix block, S is the number of repeated scalar blocks and F is the number of the full blocks. S and F satisfy the relation $\sum_{i=1}^{S} r_i + \sum_{j=1}^{F} m_j = n$, with n being the dimension of M as defined above.

For the above M and the prescribed $\mathbf{\Delta}$, $\mu_{\Delta}(M)$ is defined [9, 10] by:

$$\mu_{\Delta}(M) \stackrel{\text{def}}{=} [min \quad \bar{\sigma}(\Delta) : \Delta \in \mathbf{\Delta}, Det(I - M\Delta) = 0 \quad]^{-1} \tag{11}$$

If no Δ makes $(I - M\Delta)$ singular then $\mu_{\Delta}(M) = 0$. It is shown in [9] that the following relations hold :

$$\max_{Q \in \mathbf{Q}} \rho(QM) \leq \max_{\Delta \in \mathbf{\Delta}} \rho(\Delta M) = \mu_{\Delta}(M) \leq \inf_{D \in \mathbf{D}} \bar{\sigma}(DMD^{-1}) \tag{12}$$

where

$$\begin{aligned} \mathbf{Q} &= \{Q \in \mathbf{\Delta} \ : \ Q^*Q = I_n\} \\ \mathbf{D} &= \{diag[\Delta_1, ..., \Delta_s, d_1 I_{m1}, ..., d_F I_{mF}] \ : \\ &\quad D_i \in C^{r_i \times r_i}, D_i = D_i^* > 0 \ , \ d_j \in R, d_j > 0\} \end{aligned} \tag{13}$$

After applying a feedback controller K to the system P, defined in equations (2)–(4), as shown in Figure 1, to get $M = F_l(P, K)$, we define a Linear Fractional Transformation (LFT) [3, 4] of M with the blocks Δ_1 and Δ_2. The matrix M can be partitioned as:

$$M = \begin{bmatrix} M_{11} & M_{12} \\ M_{21} & M_{22} \end{bmatrix} \tag{14}$$

Where M_{11} is related to the parametric and model uncertainties and M_{22} is related to the system performance. The dimensions of Δ_1 and Δ_2 are compatible with the dimensions of M_{11} and M_{22} respectively. A third structure is defined as:

$$\Delta = \{ \begin{bmatrix} \Delta_1 & 0 \\ 0 & \Delta_2 \end{bmatrix} : \Delta_1 \in \mathbf{\Delta_1}, \Delta_2 \in \mathbf{\Delta_2} \} \tag{15}$$

By the small gain theorem the LFT $F_l(M, \Delta_2)$ is well posed if and only if $(I - M_{22}\Delta_2)$ is invertible, where

$$F_l(M, \Delta_2) = M_{11} + M_{12}\Delta_2(I - M_{22}\Delta_2)^{-1}M_{21} \tag{16}$$

Recalling the definition in equation (11) for μ, it can be seen that the LFT $F_l(M, \Delta_2)$ is well posed for all $\Delta_2 \in \mathbf{\Delta_2}$ if and only if $\mu_2(M_{22}) < 1$. μ_2 denotes the μ test with respect to the block structure $\mathbf{\Delta_2}$.

The μ main loop theorem [3, 4, 9] says that the following are equivalent:

$$\mu_\Delta(M) < 1 \Longleftrightarrow \mu_2(M_{22}) < 1 \qquad and \qquad \max_{\Delta_2 \in \mathbf{\Delta 2}} \{\mu_1(F_l(M, \Delta_2)) < 1\} \tag{17}$$

The μ test defined at the left is the one that captures the robust performance of the system. The software we use performs an equivalent frequency domain μ test [2]. This test enables us to analyze the robustness of a given system in the presence of a prescribed set of perturbations. The μ analysis results make it possible, by scaling the synthesized system, to improve the results from the H_∞ synthesis by making γ in equation (5) smaller. This technique of scaling the system and then synthesizing an H_∞ controller for the scaled system is the synthesis technique which will be described in the following section.

2.3 μ Synthesis.

The approach taken to μ synthesis in this paper is called D - K iteration. In D - K iteration the peak value of $\mu_\Delta(M)$ of the closed loop transfer function from w to z is minimized over all admissible controllers, i.e:

$$\min_{\substack{stabilizing \\ K(s)}} \quad \{\|F_l(P,K)\|_{\mu_\Delta}\} \tag{18}$$

where

$$\|G\|_{\mu_\Delta} \stackrel{\text{def}}{=} \max_{\omega} \quad \{\mu_\Delta[G(j\omega)]\} \tag{19}$$

We replace $\mu_\Delta(M)$ by its upper bound $\bar{\sigma}(DMD^{-1})$ and assume that $D \in \mathbf{D}$ is the appropriate scaling for the perturbed system. Recalling the upper bound in (12) and reformulating the μ synthesis objective in (18), we get

$$\min_{\substack{Stabilizing \\ K(s)}} \quad \{ \max_{\omega} \quad \{ \min_{D_\omega \in \mathbf{D}} \quad \bar{\sigma}[D_\omega F_l(P,K)_{(j\omega)} D_\omega^{-1}]\}\} \tag{20}$$

where the inner minimization is the approximation to $\mu_\Delta[F_l(P,K)_{(j\omega)}]$. D_ω is the D scaling matrix which corresponds to $F_l(P,K)_{(j\omega)}$ at the point ω. Since D_ω is chosen from $\mathbf{D}$ independently at every frequency, equation (20) can be rewritten as:

$$\min_{\substack{Stabilizing \\ K(s)}} \quad \{ \min_{D_\omega \in \mathbf{D}} \quad \{ \max_{\omega} \quad \bar{\sigma}[D_\omega F_l(P,K)_{(j\omega)} D_\omega^{-1}]\}\} \tag{21}$$

or

$$\min_{\substack{Stabilizing \\ K(s)}} \quad \{ \min_{D_\omega \in \mathbf{D}} \quad \|D_\omega F_l(P,K)_{(j\omega)} D_\omega^{-1}\|_\infty\} \tag{22}$$

Consider a real-rational, stable, minimum-phase $\hat{D}(s)$ to approximate the magnitude of D_ω over frequency. So, (22) becomes:

$$\min_{\substack{Stabilizing \\ K(s)}} \quad \{ \min_{\substack{\hat{D}(s) \\ \hat{D}(s) \in \mathbf{D}}} \quad \|\hat{D}(s) F_l(P,K)_{(j\omega)} \hat{D}(s)^{-1}\|_\infty\} \tag{23}$$

The D-K iteration procedure is defined in (23) and the steps involved are:

1. Define a stable non minimum phase function $\hat{D}(s)$ to fit the magnitude of D_ω that was computed through the μ analysis.
2. Use H_∞ synthesis to find a controller K(s) which minimizes the scaled system norm $\|\hat{D}(s)F_l(P,K)\hat{D}(s)^{-1}\|_\infty$.
3. Run the μ test. Check $\mu[F_l(P,K)]$ and build a new D_ω.
4. Go through steps 1 through 3 until no further reduction in μ is achieved.

3 Handling Qualities Requirements

The H_∞ and μ techniques require the characterization of the desired handling qualities of the aircraft to be defined in the frequency domain. Our objective is for the aircraft to satisfy level 1 handling qualities as defined in Ref. [1].

In defining the handling qualities we will use the short period linearized approximation of the aircraft dynamics given by:

$$\begin{aligned} \dot{q} &= M_q q + M_\alpha \alpha + M_\delta \delta \\ \dot{\alpha} &= q + Z_\alpha \alpha \end{aligned} \tag{24}$$

Where q is the pitch rate, α is the angle of attack, δ is the stabilizer deflection and M_q, M_α, M_δ and Z_α are the aerodynamic derivatives. The first three are the moment derivatives with respect to pitch rate, angle of attack and stabilizer deflection respectively. The fourth aerodynamic coefficient is the Z force derivative with respect to the angle of attack. The Z force due to the stabilizer deflection is neglected.

The normal acceleration at the center of gravity, in the absence of lateral velocity, roll and yaw rates, is given by:

$$n_{zcg} = \frac{Uq - \dot{w}}{g} \tag{25}$$

where U and w denote the longitudinal and the vertical velocity components of the aircraft in body axes. Using (24) and (25) we get the steady state ratio of $n_{z_{cg}}$ to α as:

$$(\frac{n_{zcg}}{\alpha})_{ss} = -\frac{Uz_\alpha}{g} \tag{26}$$

with n_z given in g units.

Assuming $\frac{\delta}{stick}$ to be constant, the transfer functions from the stick to $q, n_{z_{cg}}$ and α are:

$$\frac{q}{stick} = K_q \frac{1 - \frac{s}{z_\alpha}}{1 + \frac{2\zeta_{sp}s}{\omega_{sp}} + \frac{s^2}{\omega_{sp}^2}} \tag{27}$$

$$\frac{n_{z_{cg}}}{stick} = K_{nz} \frac{1}{1 + \frac{2\zeta_{sp}s}{\omega_{sp}} + \frac{s^2}{\omega_{sp}^2}} \tag{28}$$

$$\frac{\alpha}{stick} = K_\alpha \frac{1}{1 + \frac{2\zeta_{sp}s}{\omega_{sp}} + \frac{s^2}{\omega_{sp}^2}} \tag{29}$$

where the subscript *sp* denotes the short period approximation.

In Ref. [11] the Control Anticipation Parameter (CAP) was defined as:

$$CAP = \frac{\dot{q}_0}{n_{zss}} \tag{30}$$

The CAP is used as an indicator of aircraft maneuverability. Recalling (27) and (25) we get:

$$\begin{aligned} \frac{\dot{q}_0}{stick} &= -\frac{\omega_{sp}^2 K_q}{z_\alpha} \\ \frac{n_{zss}}{stick} &= \frac{U K_q}{g} \end{aligned} \tag{31}$$

From equation (24) we can see that $\alpha_{ss} = -\frac{q_{ss}}{z_\alpha}$ and combined with (25) we get:

$$CAP = -\frac{\omega_{sp}^2 g}{U z_\alpha} = \frac{\omega_{sp}^2}{(\frac{n_z}{\alpha})_{ss}} \tag{32}$$

In Ref. [1] the following limits are defined for level 1 performance:
For $(\frac{n_z}{\alpha})_{ss} \geq 3.5$

$$\begin{cases} 0.28 \leq CAP \leq 3.6 \\ \sqrt{0.28\frac{n_z}{\alpha}} \leq \omega_{sp} \leq \sqrt{3.6\frac{n_z}{\alpha}} \\ 0.5 \leq \zeta_{sp} \leq 1.35 \end{cases} \tag{33}$$

and for $(\frac{n_z}{\alpha})_{ss} < 3.5$

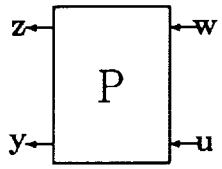

Figure 2: Basic H_∞ Formulation

$$\begin{cases} 1 & \leq & \omega_{sp} & \leq & \sqrt{3.6\frac{n_z}{\alpha}} \\ 0.5 & \leq & \zeta_{sp} & \leq & 1.35 \end{cases} \tag{34}$$

Based on recent analyses of flight simulations and tests these boundaries have been moved closer to one another as follows [12]:

For $(\frac{n_z}{\alpha})_{ss} \geq 9.0$

$$\begin{cases} 0.36 & \leq & CAP & \leq & 1.2 \\ \sqrt{0.36\frac{n_z}{\alpha}} & \leq & \omega_{sp} & \leq & \sqrt{1.2\frac{n_z}{\alpha}} \\ 0.5 & \leq & \zeta_{sp} & \leq & 1.1 \end{cases} \tag{35}$$

and For $(\frac{n_z}{\alpha})_{ss} < 9.0$

$$\begin{cases} 1.77 & \leq & \omega_{sp} & \leq & 3.2 \\ 0.5 & \leq & \zeta_{sp} & \leq & 1.1 \end{cases} \tag{36}$$

After more evaluations of handling qualities at higher angles of attack [13] larger values of the damping coefficient were found to give the best handling qualities, i.e : $\zeta_{sp} \geq 1$, and ω_{sp} is recommended to be between the lower bounds of the previous two references. Those criteria for ζ_{sp} and ω_{sp} will be used in our definition of level 1 handling qualities.

4 H_∞ Design

In order to synthesize a controller, the system under consideration is formulated as shown in Figure 2, where **w** is the disturbance vector, **z** is the error vector, **y** is the measurement vector provided to the controller, and **u** is the controller output vector. The vectors **w** and **z** are scaled so that their expected maximum absolute values are less then one. When the

controller makes $\|T_{zw}\|_\infty < 1$, the system is robust with respect to stability and the specified performance. With H_∞ synthesis, only the inputs/outputs related to the performance specifications are taken into account.

The aircraft has two pitch moment control effectors. These are the stabilizers which have a deflection limits of -24 to +10.5 *Deg* and a maximum angular rate of $\pm$ 40 *Deg/Sec*, and the Thrust Vector Control (TVC) vanes with deflection limits of -17.5 to +15 *Deg* and deflection rate limits of $\pm$ 100 *Deg/Sec.*

The controller output is a moment command that has to be divided between both effectors. The deflection command for each of the actuators is computed through a constrained optimization procedure [14]. Defining the total moment commanded by the controller to be T and the total moment produced by the control effectors to be $M_{\delta_{tvc}}\delta_{tvc} + M_{\delta_s}\delta_s$, it is clear that

$$T = M_{\delta_{tvc}}\delta_{tvc} + M_{\delta_s}\delta_s \tag{37}$$

with $M_{\delta_{tvc}}$ and M_{δ_s} being the aerodynamic moment derivatives with respect to the TVC and the stabilizer deflections respectively. We want to allocate these deflections to minimize the sum of the squares of the normalized deflections. The cost function for this constrained optimization problem is:

$$J = \frac{1}{2}\left[\left(\frac{\delta_s}{|\delta_s|_{max}}\right)^2 + \left(\frac{\delta_{tvc}}{|\delta_{tvc}|_{max}}\right)^2 \right] \tag{38}$$

Using the Lagrange Multiplier method, we define the extended cost function to be :

$$\bar{J} = J + \lambda(T - M_{\delta_{tvc}}\delta_{tvc} - M_{\delta_s}\delta_s) \tag{39}$$

Taking the derivatives with respect to δ_s, δ_{tvc} and λ and solving for δ_{tvc} and δ_s the resulting deflections are:

$$\delta_{tvc} = \frac{T/M_{\delta_{tvc}}}{1 + \frac{M_{\delta_s}}{M_{\delta_{tvc}}}\frac{|\delta_s|^2_{max}}{|\delta_{tvc}|^2_{max}}} = K_{tvc}T \tag{40}$$

$$\delta_s = \frac{T/M_{\delta_s}}{1 + \frac{M_{\delta_{tvc}}}{M_{\delta_s}}\frac{|\delta_{tvc}|^2_{max}}{|\delta_s|^2_{max}}} = K_s T \tag{41}$$

Since the TVC vanes can suffer thermal damage from the jet exhaust if they are deflected for long periods of time, there is a wash-out filter with a time constant of 1 Second in front of the TVC. The actuator dynamics are approximated by first order systems with time constants of $1/20$ second for the TVC actuators and $1/30$ second for the stabilizer actuators.

Aircraft Linear Model

As an example of our design approach, we will design a controller for the flight condition of 15000 *ft*, 20^0 angle of attack and Mach number of 0.26. The aircraft state vector for the design is $\mathbf{x} = [u,\ w,\ q,\ \theta]'$, the measurement vector is $\mathbf{y} = [\alpha,\ n_z,\ q]'$ and the control effector vector is $\mathbf{u} = [\delta_s,\ \delta_{tvc}]'$. u and w are the body longitudinal and heave velocities respectively in *ft/sec*, q is the body pitch rate in *rad/sec*, θ and α are the pitch angle and the angle of attack in *radians*. The normal acceleration in g's is denoted by n_z.

The linear model of the aircraft at the design point is :

$$\left[\begin{array}{c|c} A_{20} & B_{20} \\ \hline C_{20} & D_{20} \end{array}\right] = \left[\begin{array}{cccc|cc} 0.012 & 0.021 & -96.002 & -30.227 & -0.515 & 1.592 \\ -0.117 & -0.312 & 263.756 & -11.004 & -9.028 & -13.693 \\ 0.0003 & -0.0001 & -0.186 & 0.0 & -0.735 & -1.683 \\ 0.0 & 0.0 & 1.0 & 0.0 & 0.0 & 0.0 \\ \hline -0.001 & 0.003 & 0.0 & 0.0 & 0.0 & 0.0 \\ 0.004 & 0.010 & 0.079 & 0.0 & 0.290 & 0.426 \\ 0.0 & 0.0 & 1.0 & 0.0 & 0.0 & 0.0 \end{array}\right] \tag{42}$$

The open loop system is stable with $\omega_{ph} = 0.136$ *rad/sec*, $\omega_{sp} = 0.620$ *rad/sec*, $\zeta_{ph} = 0.019$, and $\zeta_{sp} = 0.388$. The subscript ph refers to the phugoid mode.

From (42) we see that $M_{\delta_s} = B(3,1) = -0.735$, $M_{\delta_{tvc}} = B(3,2) = -1.683$ and $Z_\alpha = A(2,2) = -0.312$.

The detailed interconnection model for the H_∞ synthesis is shown in Figure 3. This figure is an extension of Figure 2. The input and output vectors are :

$$\left\{\begin{array}{lcl} \mathbf{z} & = & [\ \tilde{\delta}_{tvc}\ \ \dot{\tilde{\delta}}_{tvc}\ \ \tilde{\delta}_s\ \ \dot{\tilde{\delta}}_s\ \ \tilde{q}\ \ \tilde{n}_z\ \ \tilde{\alpha}\ ]' \\ \mathbf{w} & = & [\ \tilde{stick}_c\ \ \tilde{n}_\alpha\ \ \tilde{n}_{n_z}\ \ \tilde{n}_q\ ]' \\ \mathbf{y} & = & [\ stick_c\ \ q_m\ \ n_{z_m}\ \ \alpha_m\ ]' \\ \mathbf{u} & = & T \end{array}\right. \tag{43}$$

The first two components of $\mathbf{z}$ are the scaled TVC deflection and deflection rate and the next two components are the scaled stabilizer deflection and deflection rate. The last three

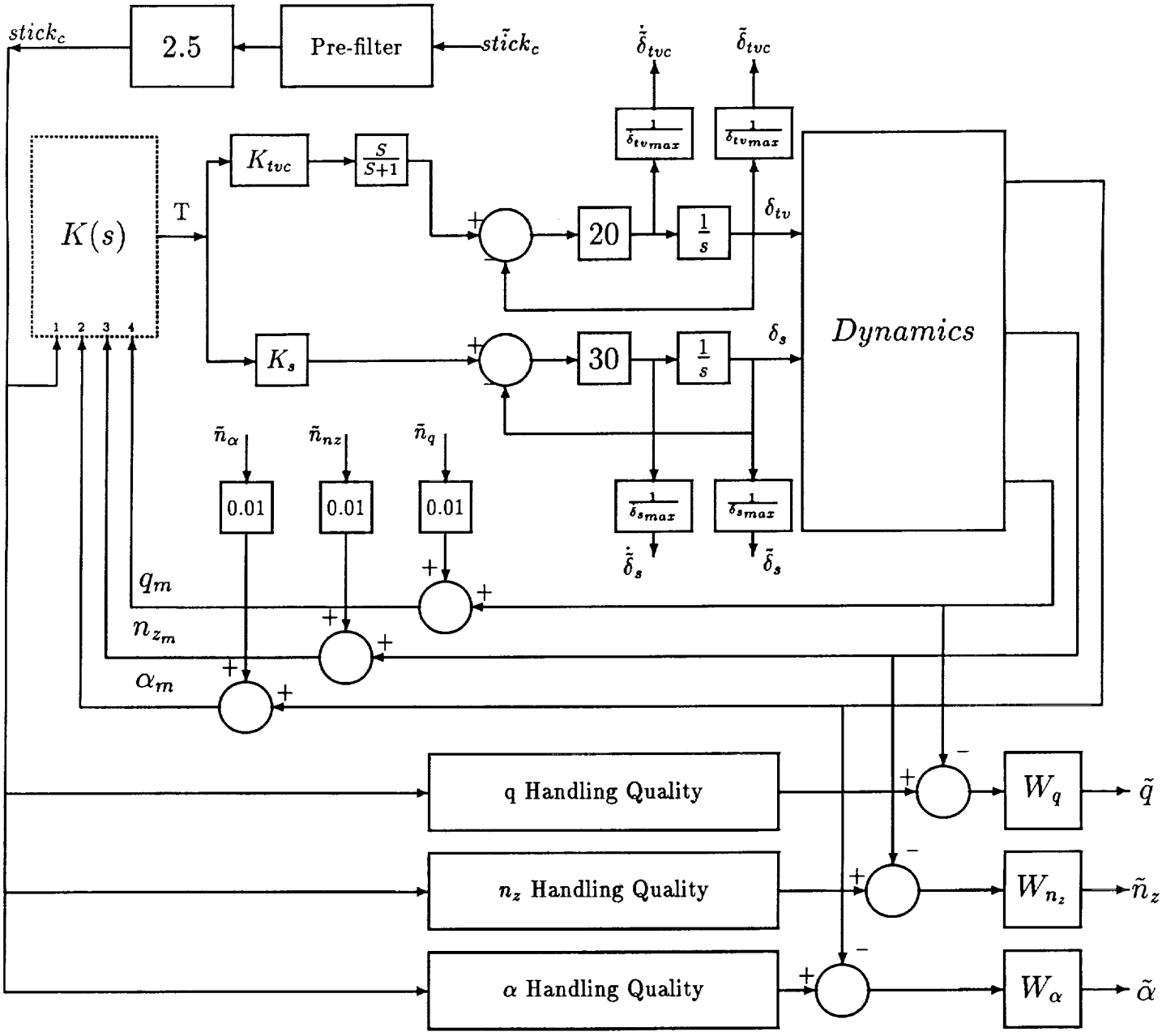

Figure 3: Interconnection Structure for H_∞ Synthesis

components are the scaled errors in q , n_z and α respectively. The **w** components are the scaled stick input and the additive noise in the α , n_z and q measurements. The vector **y** is composed of the actual stick deflection and sensor outputs. The vector **u** is the controller output.

The system is formulated so that all three handling quality criteria can be included in the synthesis. In this example we only optimize with respect to the angular rate, q. That is we want the angular rate to track the pilot stick input. For this case the weighting functions,W_{n_z} and W_α are set to very small numbers so they will not effect the design objective of satisfying the q handling quality criterion. From equations (27–29), the handling qualities parameters: ω_{sp},K_q,K_{n_z} and K_α are related to the aircraft linearized model. According to the relationship given in (26) $(\frac{n_{zcg}}{\alpha})_{ss} = 2.5$ and from section 3 we choose ω_{sp} and ζ_{sp} to be 1 *rad/sec* and 1 respectively. Our basic requirement is for the aircraft to have the capability of performing an acceleration of 1 g due to 1 *inch* of stick input. This requirement results in K_{n_z} in equation (28) to be 1 *g/inch*. Using (25) for $\dot{w} = 0$ $K_q = K_{n_z}\frac{g}{U} = 0.115\ \frac{rad}{sec}/inch.$ From the second equation in (24), for $\dot{\alpha} = 0$ we get $K_\alpha = \frac{K_q}{Z_\alpha} = 0.368\ rad/inch.$

A point to remember is that the handling quality transfer functions are related to the short period approximation of the aircraft. For the actual aircraft which includes the phugoid mode as well as the short period, the actual steady state values of q and n_z for a given stick input are zero.

The inputs to the weighting functions: W_q, W_{n_z} and W_α are the differences between the desired output from the handling quality model, and the actual output from the aircraft model. We would like the actual transfer function between the stick and pitch rate to be as close as possible to the handling quality transfer function between the stick and desired pitch rate, defined in (27). The weighting which defines how well we want to follow the handling quality transfer function is W_q. We define W_q to be:

$$W_q = 57.3\frac{1+\frac{s}{100}}{1+\frac{s}{3}} \tag{44}$$

This weighting function defines an allowed tracking error of 1 *Deg/Sec* up to the bandwidth of 3 *Rad/Sec*. Above 3 *Rad/Sec*, the error is allowed to grow by allowing W_q to decrease until the frequency of 100 *Rad/Sec*. We allow larger errors in this frequency range since we are not interested in tracking inputs at frequencies greater then 3 *Rad/Sec*. The weighting function does not decrease above 100 *Rad/Sec* in order to limit high gains at high frequency so that high frequency elastic modes effects are not excited. Since we put no constraints on n_z and α errors, we set W_{n_z} and W_α to be very small, so the design will not be affected by

n_z and α handling quality requirements.

Since n_z and α handling quality requirements are derived from the same short period approximation as is the q handling quality requirement, we would expect that as long as the short period equations approximation is valid, a control law which satisfies the q handling quality requirement also does a reasonable job of satisfying the n_z and α handling quality requirements. This is the case at lower values of angle of attack where there is good separation between phugoid and short period modes. As the angle of attack increases, the phugoid and short period frequencies approach one another and satisfaction of one handling quality requirement does not mean that the others are also satisfied.

The noise assumed through the design is a white noise with zero mean and with the following spectral density components : 0.01 $Rad/\sqrt{\frac{Rad}{Sec}}$ in α measurement, 0.01 $g/\sqrt{\frac{Rad}{Sec}}$ in n_z measurement and 0.01 $\frac{Rad}{Sec}/\sqrt{\frac{Rad}{Sec}}$ in q measurement. The maximum stick deflection for which the design was performed is 2.5 *inches*, the stabilizers and TVC maximum deflections, $|\delta_s|_{max}$ and $|\delta_{tvc}|_{max}$, are 10.5 *Deg* and 16.0 *Deg*, and their maximum rates, $|\dot{\delta}_s|_{max}$ and $|\dot{\delta}_{tvc}|_{max}$, are 40 *Deg/Sec* and 100 *Deg/Sec* respectively. Recalling equations (40) and (41) together with the aerodynamic coefficients and the above maximum deflections we get that $K_{tvc} = -0.500$ and $K_s = -0.215$.

Since the H_∞ synthesis is a frequency domain design technique, the stick deflection should also be characterized in the frequency domain. It is assumed that it takes the pilot at least 2 *Seconds* to deflect the stick from zero to its maximum value of +2.5 *inches* back through zero to its minimum deflection of -2.5 *inches* and then back to zero. This corresponds to a bandwidth of 3.14 *Rad/Sec.* Since the force which the pilot applies is proportional to the stick acceleration, the transfer function from the pilot force input to the actual stick deflection is a second order system with a bandwidth of 3.14 *Rad/Sec.* This transfer function is realized by the $pre - filter$ block in Figure 3. The transfer function defined for $pre - filter$ is :

$$pre - filter = \frac{9.86}{s^2 + 6.28s + 9.86} \tag{45}$$

The above models were used in our initial control law design. We first designed our control laws using a short period approximation of the aircraft dynamics. This resulted in a small value for γ, but when these control laws were applied to the full aircraft dynamics which included the phugoid, very poor performance resulted. Next we decided to include a phugoid model in our handling quality requirements. This allowed us to keep γ small and provided excellent performance when the control laws were used with the full aircraft model. In addition, if the handling quality model only contains the aircraft short period approximation,

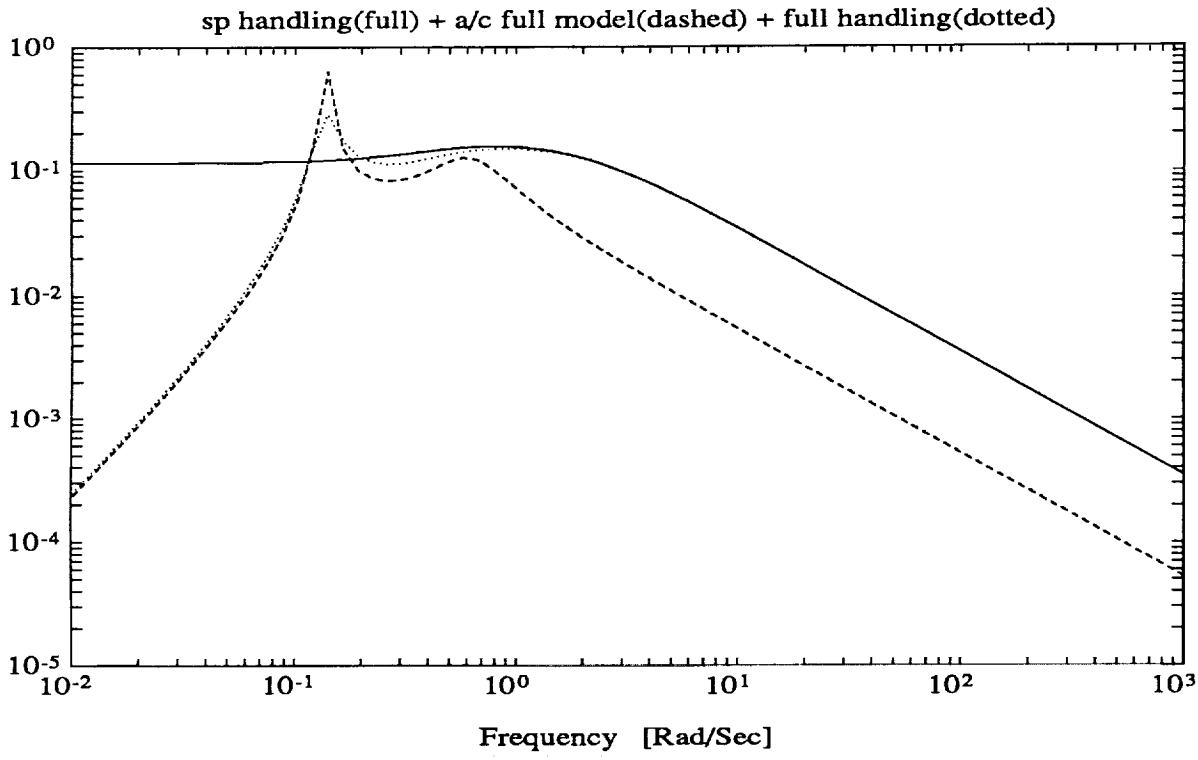

Figure 4: $\frac{q}{stick}$ transfer functions

the resulting control law design cannot directly modify the phugoid mode. With our approach we can stabilize unstable phugoid poles and increase their damping if needed.

The inclusion of a phugoid mode in the handling quality requirement is done by curve fitting the aircraft phugoid approximation at low frequency to the short period handling quality specification. Because of the wash out filter in front of the TVC input, only the stabilizers are effective at frequencies up to the phugoid frequency. Allowing 10.5 *Deg* of stabilizer deflection for maximum stick deflection of 2.5 *Inches* we get the low frequency relationship:

$$\frac{q}{stick} = 0.072 \frac{q}{\delta_s} \tag{46}$$

The curve fitting and modification to the handling quality specification is shown in Figure 4. Note the increased damping of the phugoid mode in the handling quality model compared with the actual aircraft transfer function. The maximum singular value over frequency of the closed loop transfer function of the system given in Figure 3 is shown in Figure 5. The fact that the maximum singular value is less then one means that the system performs according to the specification in the different weighting functions that were defined in the H_∞ synthesis

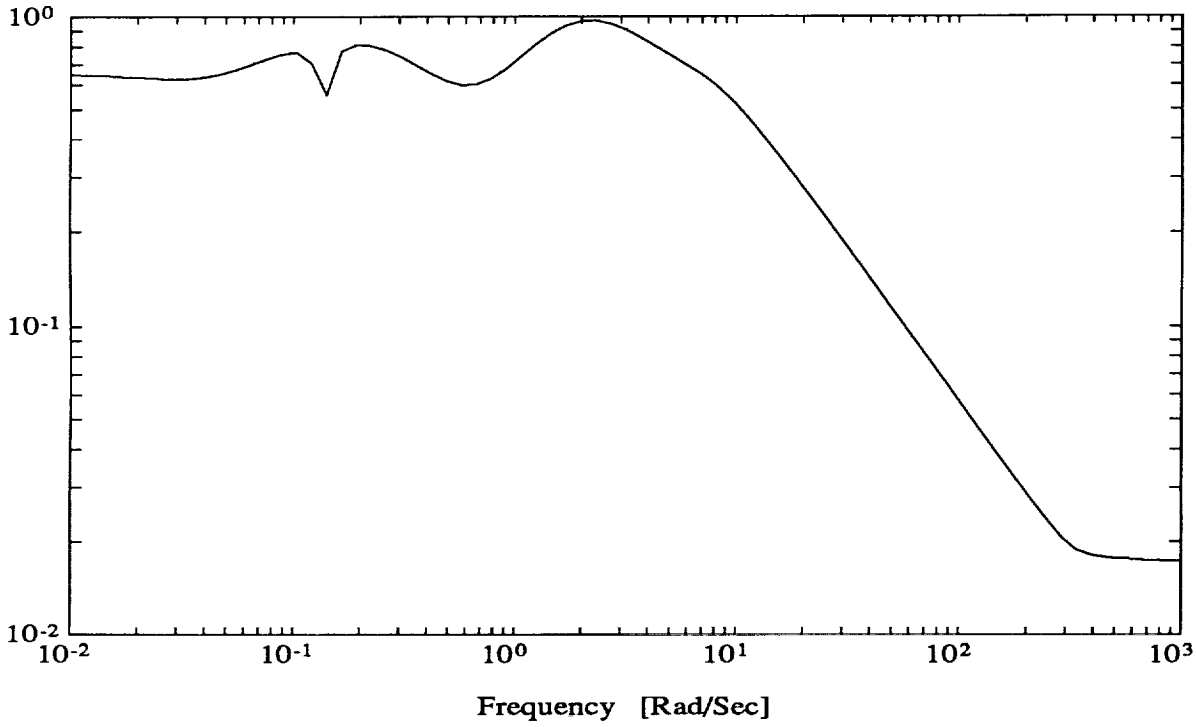

Figure 5: Closed loop maximum singular value

formulation.

Further analyses were done to verify the results. The first was a time simulation of the closed loop system applied to the linearized aircraft model. The results are shown in Figure 6. The input to the system is a stick doublet shown in Figure 6h. The stick amplitude is 2.5 *inches*. In the figures [variable_hq] stands for the response of the handling quality model to the stick input, and [dvariable] is the difference between the response of the closed loop linearized aircraft model and the handling quality response. Figures 6a and 6b indicate that the actuators are almost at their limits, and Figures 6c and 6g show that the actual pitch attitude and rate are extremely close to those defined by the handling quality transfer function. Also Figures 6e and 6f show that we follow the desired handling quality specifications for α and n_z even though those were given very small weightings in our H_∞ design procedure. Figure 6d indicates that we do not follow the flight path angle from the handling quality model very well initially, however the flight path angle is a long period variable whereas our objective was to improve short period response. Also as time increases, the flight path angles from the handling quality specification and the aircraft are essentially the same. Thus based on linear models our H_∞ design is successful.

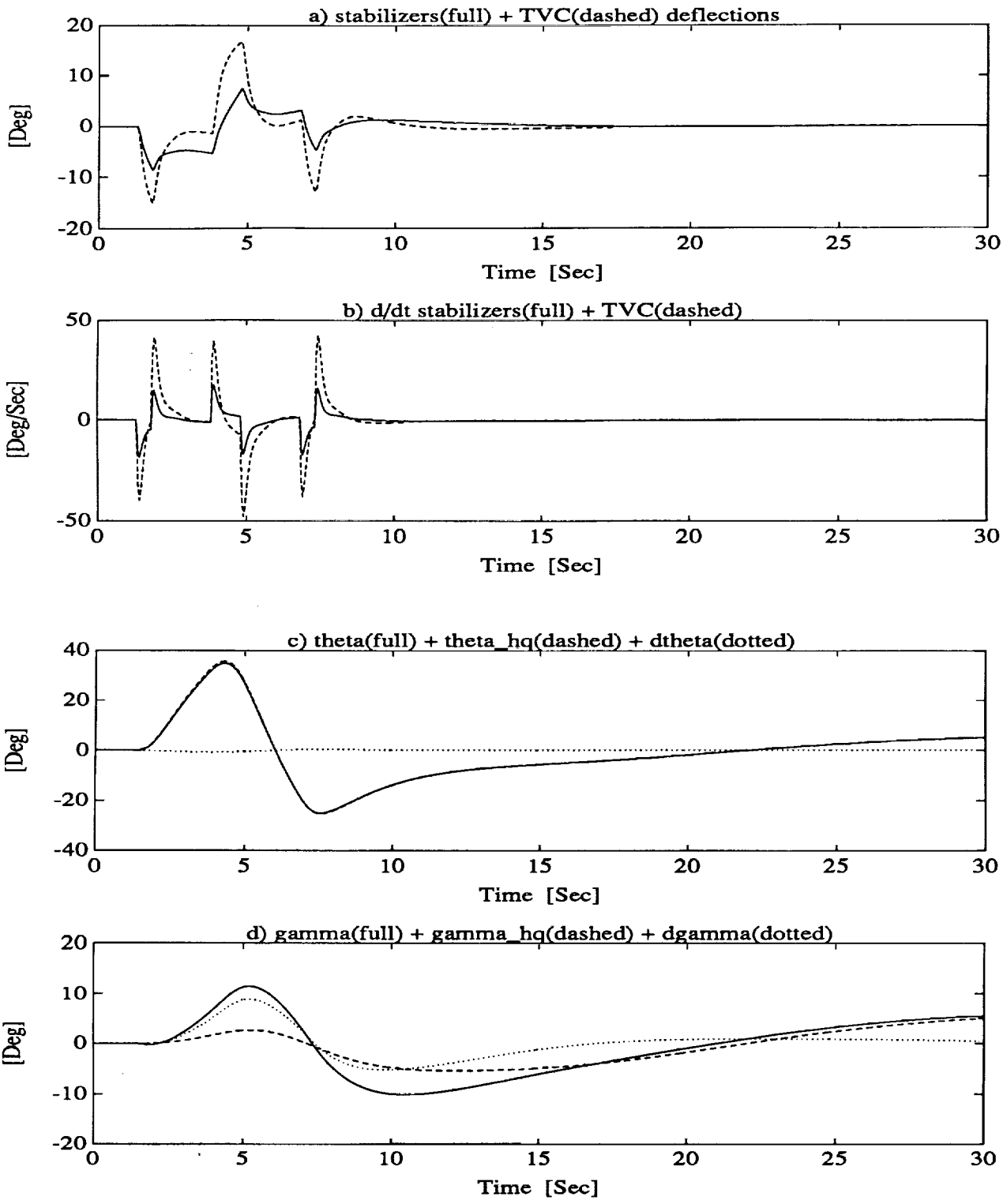

Figure 6: Time response of the linear simulation with the H_∞ controller

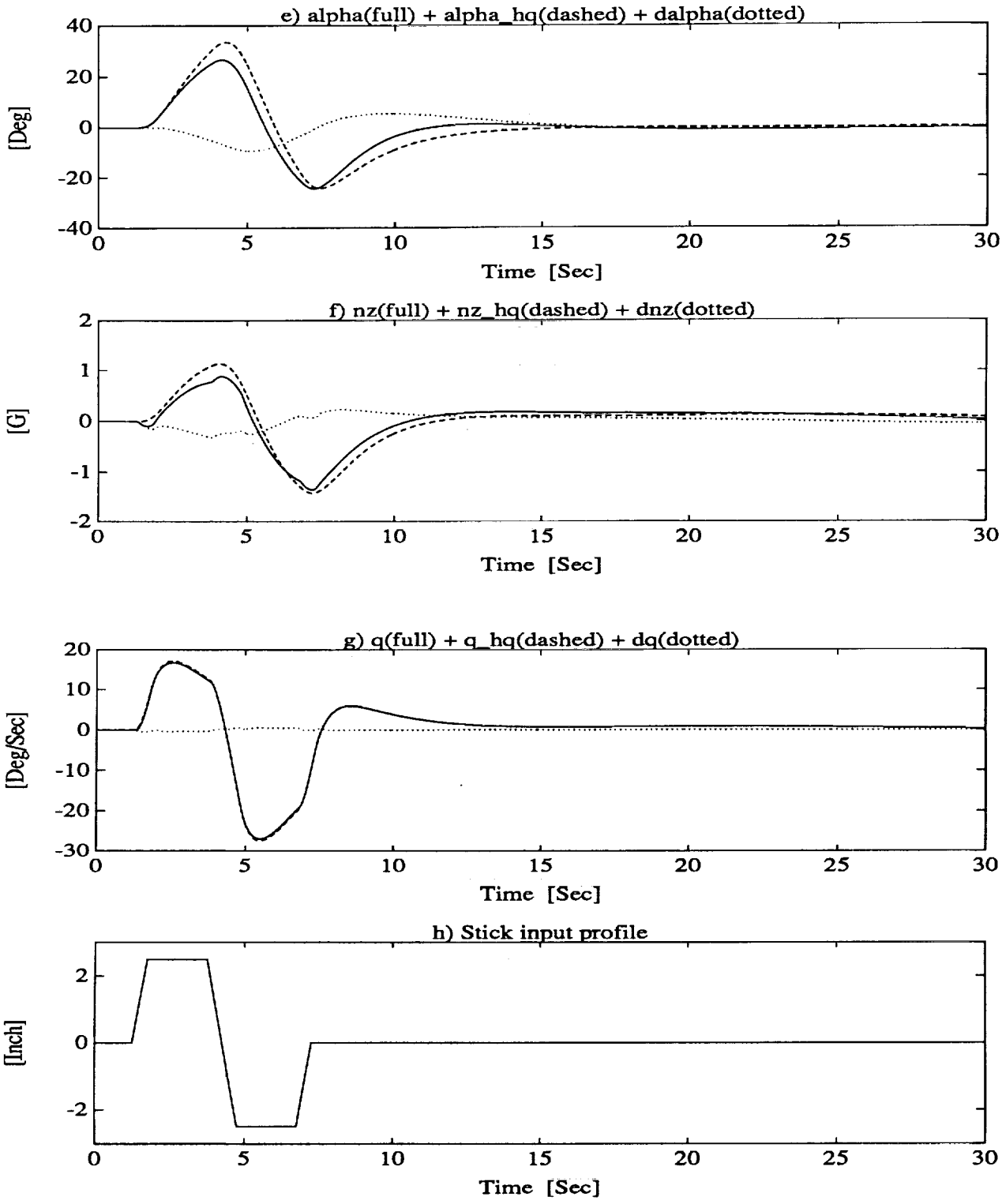

Figure 6: Time response of the linear simulation with the H_∞ controller

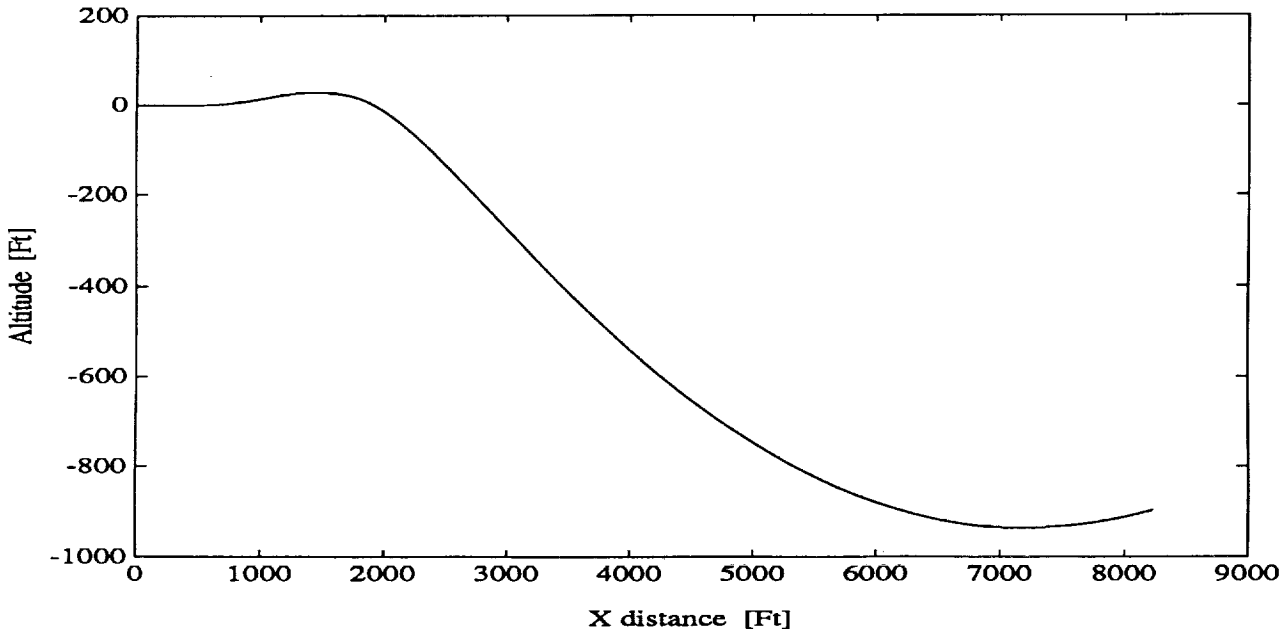

Figure 7: Aircraft trajectory on X - Z plane

Next step in analyzing the H_∞ controller is by inserting it into the full nonlinear simulation of the HARV. The doublet stick input is identical to that for the linear simulation. The aircraft trajectory in x-z plane is shown in Figure 7 and its Mach number is presented in Figure 8. The ordinate in Figure 7 shows the deviation from the initial altitude of 15000 *ft*. The Mach number is not continuous because of the way its computation is performed as a function of the angle of attack in the simulation.

It can be seen that the aircraft climbs slightly and then loses about 1000 *ft* at altitude. It then starts to climb again. Figure 8 indicates a decrease in Mach number with the initial climb followed by an increase as the aircraft descends. Figures 7 and 8 illustrate the classical damped phugoid mode.

Figure 9 includes the remainder of the aircraft responses. Figure 9a shows the deflection of the stabilizers and the TVC vanes. Both reach their maximum values during the maneuver. At this simulation no limit was enforced on the TVC vanes so they were slightly above the actual limit. Figure 9b shows the stabilizer deflection rate. The TVC deflection rate is not an output of the simulation so it is not shown. The deflection rates do not reach their maximum values. Thus the maneuver is limited by the control effector deflections rather then deflection rates. Figure 9c shows the pitch angle, θ , from the nonlinear simulation and from the handling qualities models. (note that both θ and α from the handling qualities

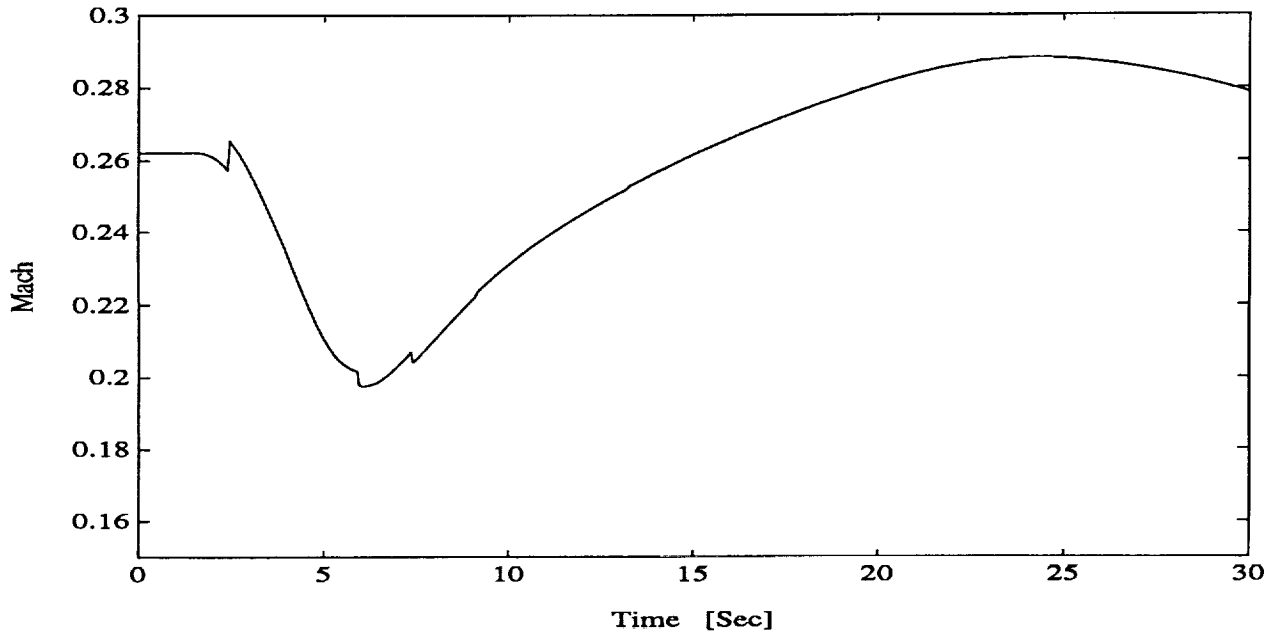

Figure 8: Mach number as a function of time

model have been increased by steady state values of 20 *Deg* which are the equilibrium values of these variables for this flight condition). The pitch angle from the nonlinear simulation tracks the pitch angle from the handling quality model very closely even though angular excursion of approximately 40 *Deg* from the equilibrium are encountered. The flight path angle from the handling quality model is shown in Figure 9d. As in the linear case the handling quality flight path angle is not tracked very well, however, tracking of flight path angle was not one of our design objectives. Figure 9e shows excellent tracking of angle of attack. Normal acceleration is tracked less well. This could be because there is lateral motion in the nonlinear simulation which effects the measured normal acceleration. The handling quality model is based on the assumption that there is no lateral motion. Figure 9g shows that the pitch rate from the nonlinear simulation tracks the handling quality model very well and Figure 9h shows that the pitch rate also tracks the stick input profile well. Since the control law was designed to provide pitch rate tracking of the stick input, the H_∞ control meets this design criterion very well.

If robustness issues are ignored we see that the H_∞ design gives us good performance and the nonlinear results are very similar to the linear results for relatively large angle of attack changes. The H_∞ design is very conservative in terms of stability robustness since error models are not included explicitly in the synthesis procedure. The μ synthesis procedure

includes error models and is the subject of the next section.

5 μ synthesis controller

The μ synthesis controller was designed to compensate for the following four sources of uncertainty in the math model of the aircraft:

1. Parametric uncertainties in the linear aircraft A matrix.
2. Actuator effectiveness uncertainty.
3. Measurement uncertainty.
4. Input uncertainty.

The first uncertainty will be presented as an LFT while the others will be treated as multiplicative uncertainties. All the uncertainties will be translated into an extended LFT in order to perform the μ synthesis. The synthesis software available at this time assumes all the perturbations and uncertainties are complex. A real μ analysis will be presented along with the complex μ analysis and we shall see that both are very close to each other. This indicates that very little performance is lost by modeling uncertainties as complex functions.

Since our controller will not be scheduled on any of the measurements, we shall carry out our design for a small range of Mach number and angle of attack variations.

The three points in the flight envelope for which the controller will be synthesized are: 1) H = 15000 *ft*, Mach = 0.291, $\alpha = 15^0$ 2) H = 15000 *ft*, Mach = 0.258, $\alpha = 20^0$ and 3) H = 15000 *ft*, Mach = 0.246, $\alpha = 25^0$

The linear model at 20^0 is given by equation (42) while the other two linear models are given below.

At H = 15000, Mach = 0.291 and $\alpha = 15^0$ the linear model is:

$$\left[\begin{array}{c|c} A_{15} & B_{15} \\ \hline C_{15} & D_{15} \end{array}\right] = \left[\begin{array}{cccc|cc} 0.004 & 0.025 & -78.939 & -31.071 & -1.271 & 2.771 \\ -0.132 & -0.315 & 294.589 & -8.327 & -12.033 & -15.116 \\ 0.0004 & -0.0021 & -0.199 & 0.0 & -0.862 & -1.866 \\ 0.0 & 0.0 & 1.0 & 0.0 & 0.0 & 0.0 \\ \hline -0.001 & 0.003 & 0.0 & 0.0 & 0.0 & 0.0 \\ 0.004 & 0.010 & 0.091 & 0.0 & 0.376 & 0.470 \\ 0.0 & 0.0 & 1.0 & 0.0 & 0.0 & 0.0 \end{array}\right] \quad (47)$$

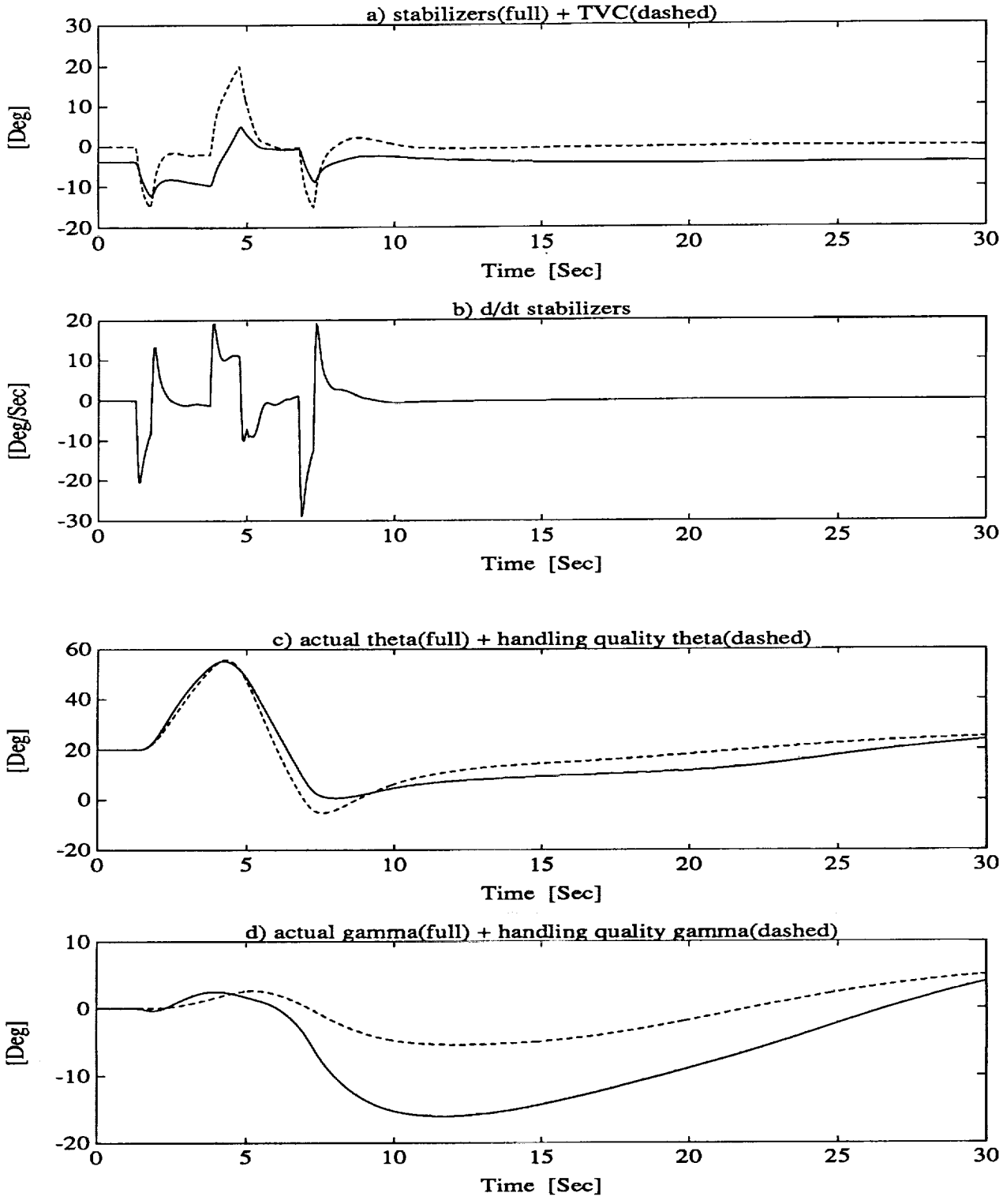

Figure 9: Time response of the nonlinear simulation with the H_∞ controller

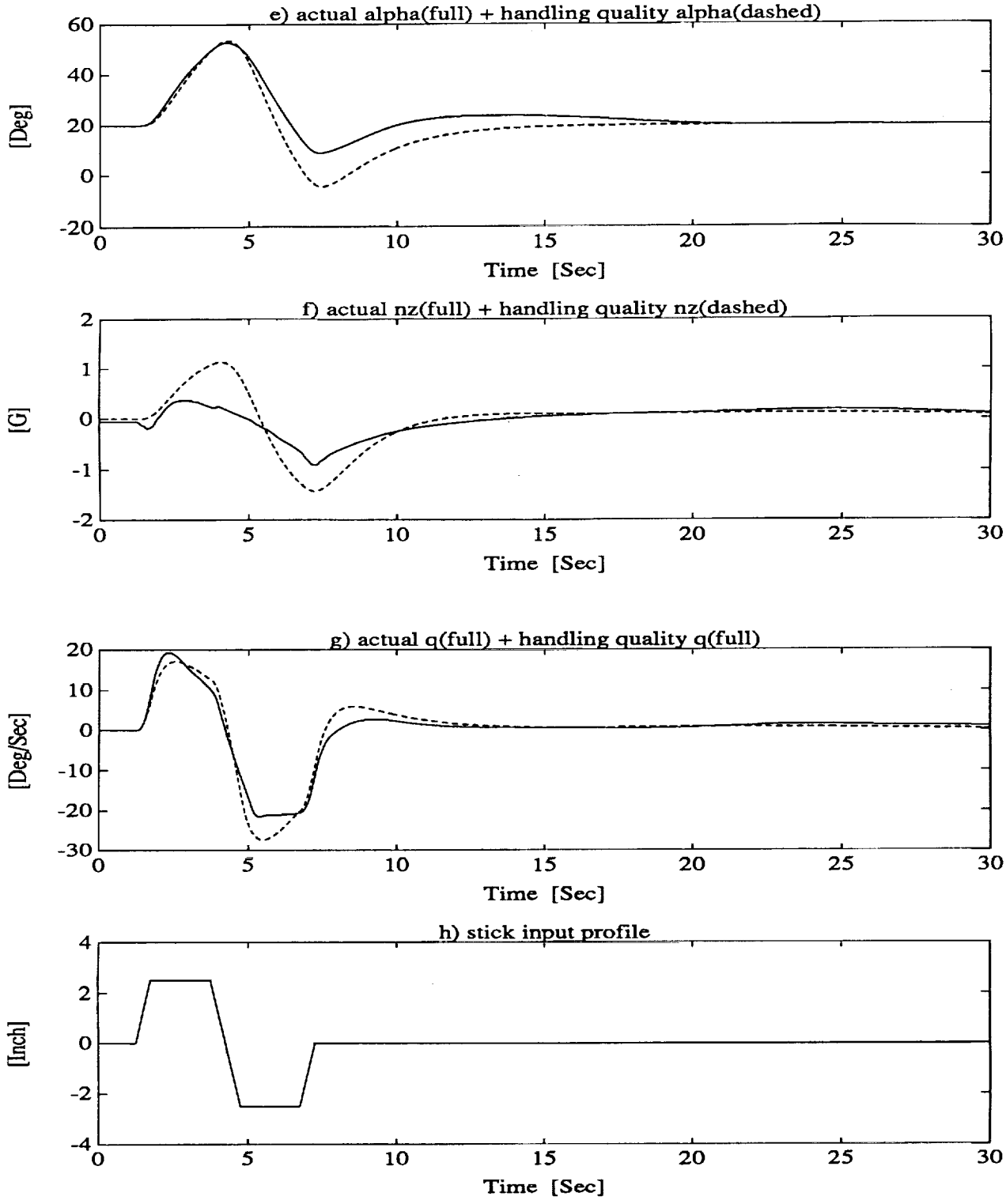

Figure 9: Time response of the nonlinear simulation with the H_∞ controller

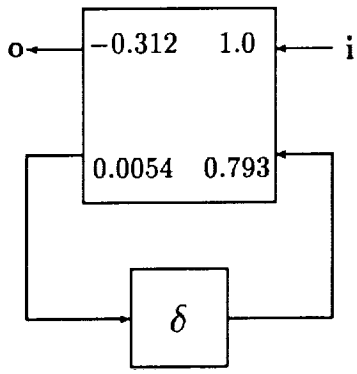

Figure 10: A_{22} variations as an LFT

At H = 15000, Mach = 0.246 and $\alpha = 25^0$ the linear model is:

$$\left[\begin{array}{c|c} A_{25} & B_{25} \\ \hline C_{25} & D_{25} \end{array}\right] = \left[\begin{array}{cccc|cc} 0.024 & 0.002 & -109.202 & -29.153 & -1.520 & 0.432 \\ -0.116 & -0.286 & 234.186 & -13.596 & -7.529 & -11.188 \\ 0.0002 & -0.0001 & -0.167 & 0.0 & -0.604 & -1.367 \\ 0.0 & 0.0 & 1.0 & 0.0 & 0.0 & 0.0 \\ \hline -0.002 & 0.004 & 0.0 & 0.0 & 0.0 & 0.0 \\ 0.004 & 0.009 & 0.070 & 0.0 & 0.239 & 0.348 \\ 0.0 & 0.0 & 1.0 & 0.0 & 0.0 & 0.0 \end{array}\right] \quad (48)$$

The elements, A_{22} A_{23} A_{32} and A_{33} , in each of the above linear models define the short period mode. The nominal system for the design is for the 20^0 flight condition.

As an example of modeling the parametric variations in A let us examine how A_{22} variations can be brought into LFT form. We shall define $A_{22_{nom}} = -0.312$, $A_{22_{min}} = -0.315$ and $A_{22_{max}} = -0.286$. The variations in A_{22} are shown in Figure 10 in LFT form. The relation of A_{22} to δ is:

$$A_{22} = T_{oi} = -0.312 + \frac{0.0054\delta}{1 - 0.793\delta} \quad (49)$$

One can check that for $\delta = 1$ $T_{oi} = -0.286$, for $\delta = 0$ $T_{oi} = -0.312$ and for $\delta = -1$ $T_{oi} = -0.315$. Variations in A_{23}, A_{32} and A_{33} are modeled in a similar manner. Variations in the remaining elements of A are not considered in the design.

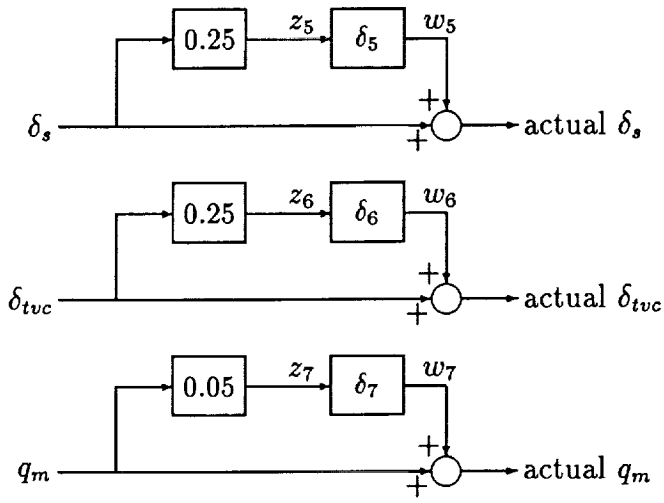

Figure 11: δ_s , δ_{tvc} and q_m variations.

Putting the variations of the four elements in A which are related to the short period mode into an LFT form gives us the following structure:

$$\left[\begin{array}{c} \dot{u} \\ \dot{w} \\ \dot{\theta} \\ \dot{q} \\ \hline z_1 \\ z_2 \\ z_3 \\ z_4 \\ \hline \mathbf{y} \end{array}\right] = \left[\begin{array}{cccc|cccc|c} & & A_{20} & & 0 & 0 & 0 & 0 & \\ & & & & 1 & 1 & 0 & 0 & \\ & & & & 0 & 0 & 1 & 1 & B_{20} \\ & & & & 0 & 0 & 0 & 0 & \\ \hline 0 & 0.0054 & 0 & 0 & 0.793 & 0 & 0 & 0 & 0 \\ 0 & 0 & 30.175 & 0 & 0 & 0.0203 & 0 & 0 & 0 \\ 0 & 0.001 & 0 & 0 & 0 & 0 & 0.0846 & 0 & 0 \\ 0 & 0 & 0.0161 & 0 & 0 & 0 & 0 & 0.1561 & 0 \\ \hline & & C_{20} & & 0 & 0 & 0 & 0 & D_{20} \end{array}\right] \left[\begin{array}{c} u \\ w \\ \theta \\ q \\ \hline w_1 \\ w_2 \\ w_3 \\ w_4 \\ \hline \mathbf{u} \end{array}\right] \quad (50)$$

Where z_1 w_1 are related to A_{22} variations, z_2 w_2 to A_{23} variations, z_3 w_3 to A_{32} variations and z_4 w_4 to A_{33} variations. Every z_i is connected to its corresponding w_i through $|\delta_i| \leq 1$ where i = 1,2,3,4.

Assuming a 25% multiplicative uncertainty in the effectiveness of the control effectors and a 5% multiplicative uncertainty in the measurement scaling, the blocks that should be inserted into Figure 3 are shown in Figure 11. The δ_s and δ_{tvc} blocks should be inserted at the aircraft dynamics input, and q_m at the controller input.

Input uncertainty was used for modeling the uncertainty of the system dynamics at both low and high frequency. The input uncertainty model is based on the assumptions that 1) the uncertainty at low frequencies is 20% 2) the first elastic mode is at 30 *Rad/Sec* and

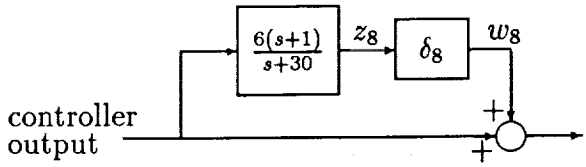

Figure 12: Input uncertainty structure.

3) the elastic modes add 600% of uncertainty to the system dynamics. The resulting input uncertainty model was selected as:

$$input\ \ uncertainty\ =\ \frac{6(s+1)}{s+30} \tag{51}$$

With this uncertainty model, the structure shown in Figure 12 has to be inserted after the controller output in Figure 3. Taking all the above uncertainties and perturbations into consideration, we define a new system interconnection in the format of Figure 2. In this case **y** and **u** are the same as those defined in equation (43) for the H_∞ synthesis. The **z** and **w** vectors for the μ synthesis are:

$$\mathbf{z} = [z_1\ z_2\ z_3\ z_4\ z_5\ z_6\ z_7\ z_8\ \tilde{\delta}_{tvc}\ \dot{\tilde{\delta}}_{tvc}\ \tilde{\delta}_s\ \dot{\tilde{\delta}}_s\ \tilde{q}\ \tilde{n}_z\ \tilde{\alpha}\ ]' \tag{52}$$

$$\mathbf{w} = [w_1\ w_2\ w_3\ w_4\ w_5\ w_6\ w_7\ w_8\ \tilde{stick}_c\ \tilde{n}_\alpha\ \tilde{n}_{n_z}\ \tilde{n}_q\ ]' \tag{53}$$

Note the difference in the dimensions of **w** and **z** compared to those defined in equation (43) for the H_∞ synthesis. The additional inputs/outputs are necessary for addressing stability robustness.

Using the above definitions for all the inputs and outputs of the basic interconnection structure shown in Figure 2, we went through the D-K iterations. Starting with the first γ of the H_∞ design to be 25 and the first μ value of the μ analysis to be 10 we went through 7 D-K iterations to get the final and lowest μ we could achieve.

The final μ achieved is shown as a function of frequency in Figure 13. The full line is the upper bound for the complex μ analysis. Its maximum is 2.77. The dashed line is the upper bound for the real μ analysis, and its maximum is 2.72.

The μ controller was applied to the three linear models of the aircraft at $\alpha = 15^0$, $\alpha = 20^0$ and $\alpha = 25^0$. Only one unstable pole resulted. This was for $\alpha = 25^0$ and it had a very slow time constant of 1250 *Sec*. Using the H_∞ controller with the same linear models we get an unstable pole with a time constant of about 100 *Sec* at $\alpha = 25^0$.

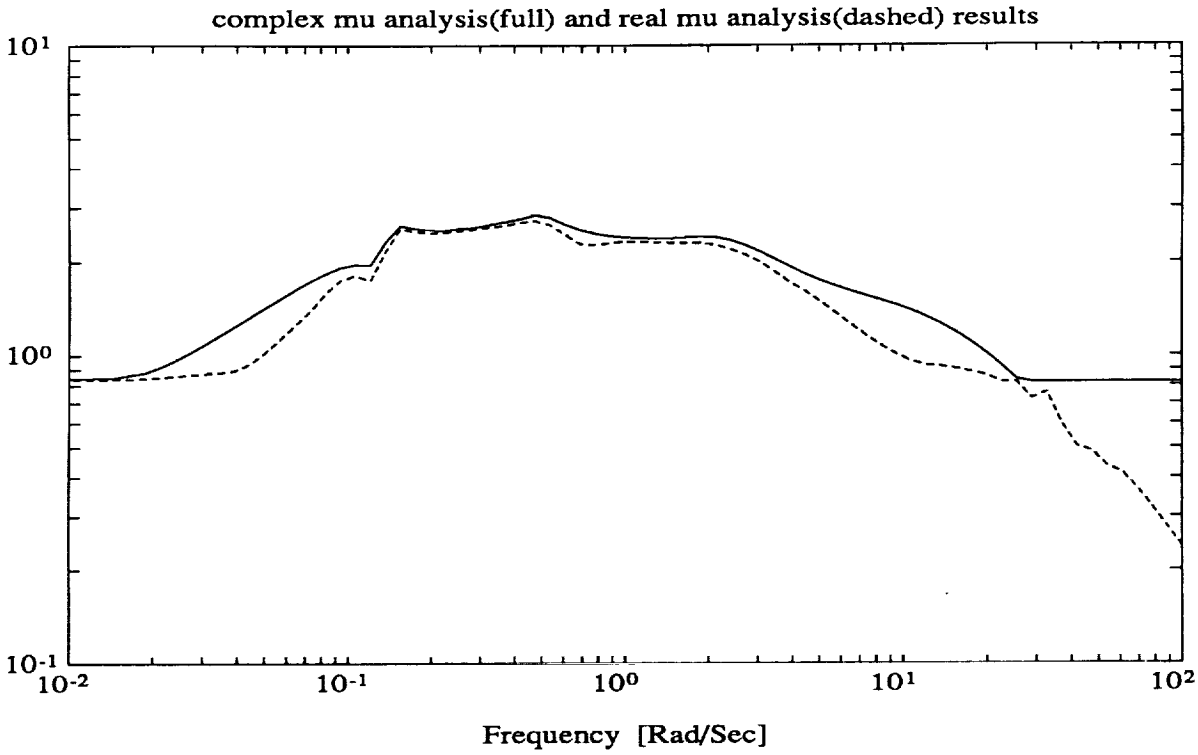

Figure 13: complex and real μ analyses results.

To test for the μ controller performance, 6 linear simulations were done. 3 with the μ controller and 3 with the H_∞ controller. Each controller was simulated with the aircraft linear models at 15^0, 20^0 and 25^0. The results of comparing the pitch rate, q, in all the cases are presented in Figure 14. The only point the H_∞ controller has a better response is at the nominal design condition at $\alpha = 20^0$. At the other two points the μ controller is better then the H_∞ controller in the sense that its settling time is smaller, its response is less oscillatory and it can better track the handling quality response.

The μ controller that was synthesized has 111 states. Using a system balanced model reduction we designed a 25 state controller with the upper bound on μ being 2.82. This reduced order controller was inserted into the full nonlinear HARV simulation. The nonlinear results along with the handling qualities responses are given in Figure 15.

Even though no major differences can be noticed between both nonlinear simulations – the one with the H_∞ controller, Figure 9, and the other with the μ controller, Figure 15 – the μ controller is superior to the H_∞ controller from the linear analyses. As mentioned before, the closed loop system with the μ controller has a much slower unstable mode then the closed loop system with the H_∞ controller. The system with the μ controller performs better at all points other than the nominal design point.

In the above we showed how we succeeded in synthesizing a μ controller that addresses the stability robustness and at the same time provides performance close to the specifications with the three linear models as well as with the nonlinear simulation. When adding a scheduling algorithm on α or on the Mach number, the maximum value of μ should be lower then 2.77. Hopefully this will result in μ close to one.

Adding the variations in the other elements of A matrices to capture the phugoid modes variations will make the D-K iteration longer. This is not necessary as long as the phugoid modes are stable, as they are in our case.

6 Controllers Comparison

Before implementing a dynamic inversion control law on the HARV, we are synthesizing a μ controller that will follow the α handling quality transfer function as defined in equation (29). The angle of attack handling quality transfer function will be followed at the high angles of attack regime.

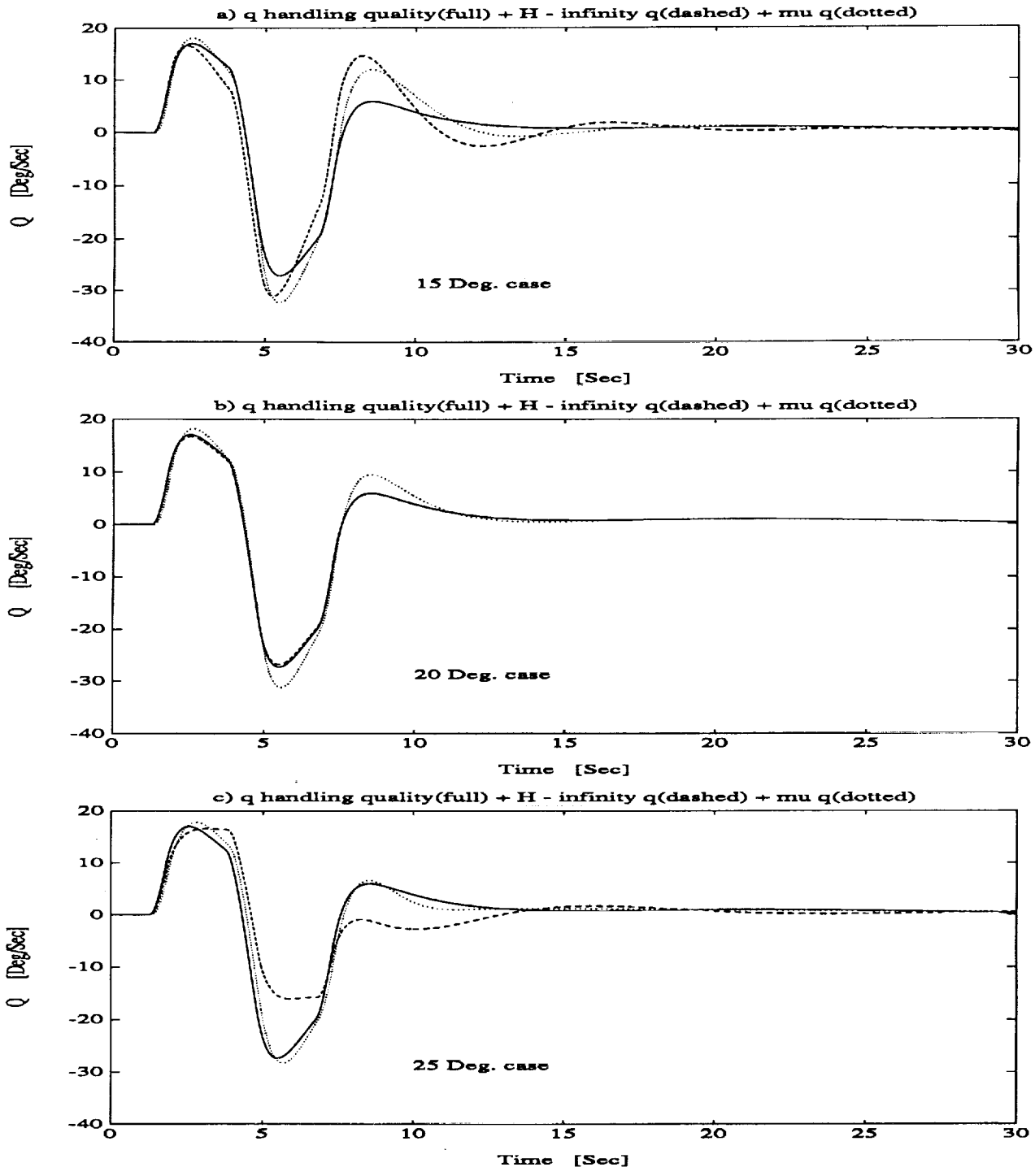

Figure 14: Comparing H_∞ and μ controllers performances

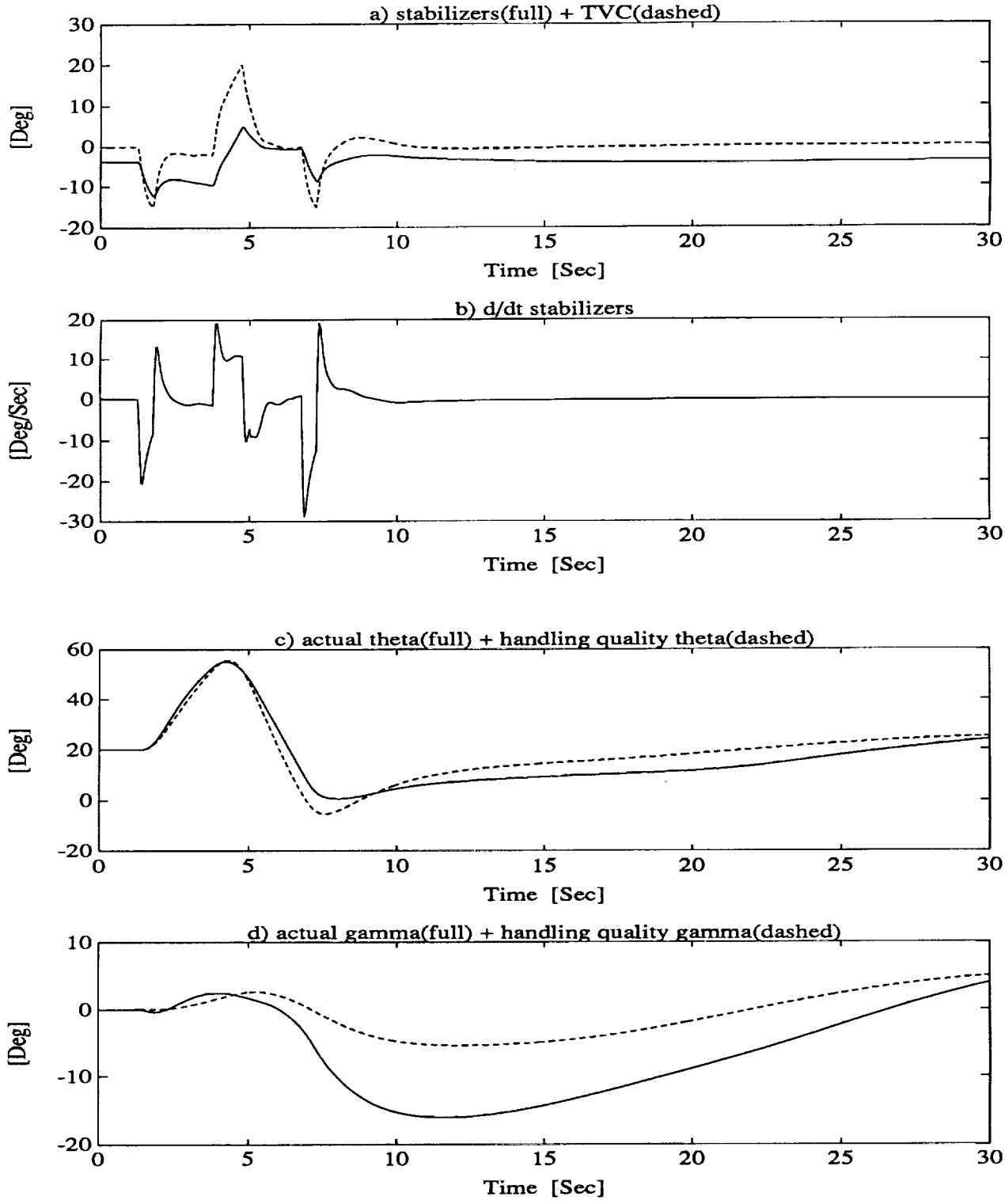

Figure 15: Time response of the nonlinear simulation with μ controller

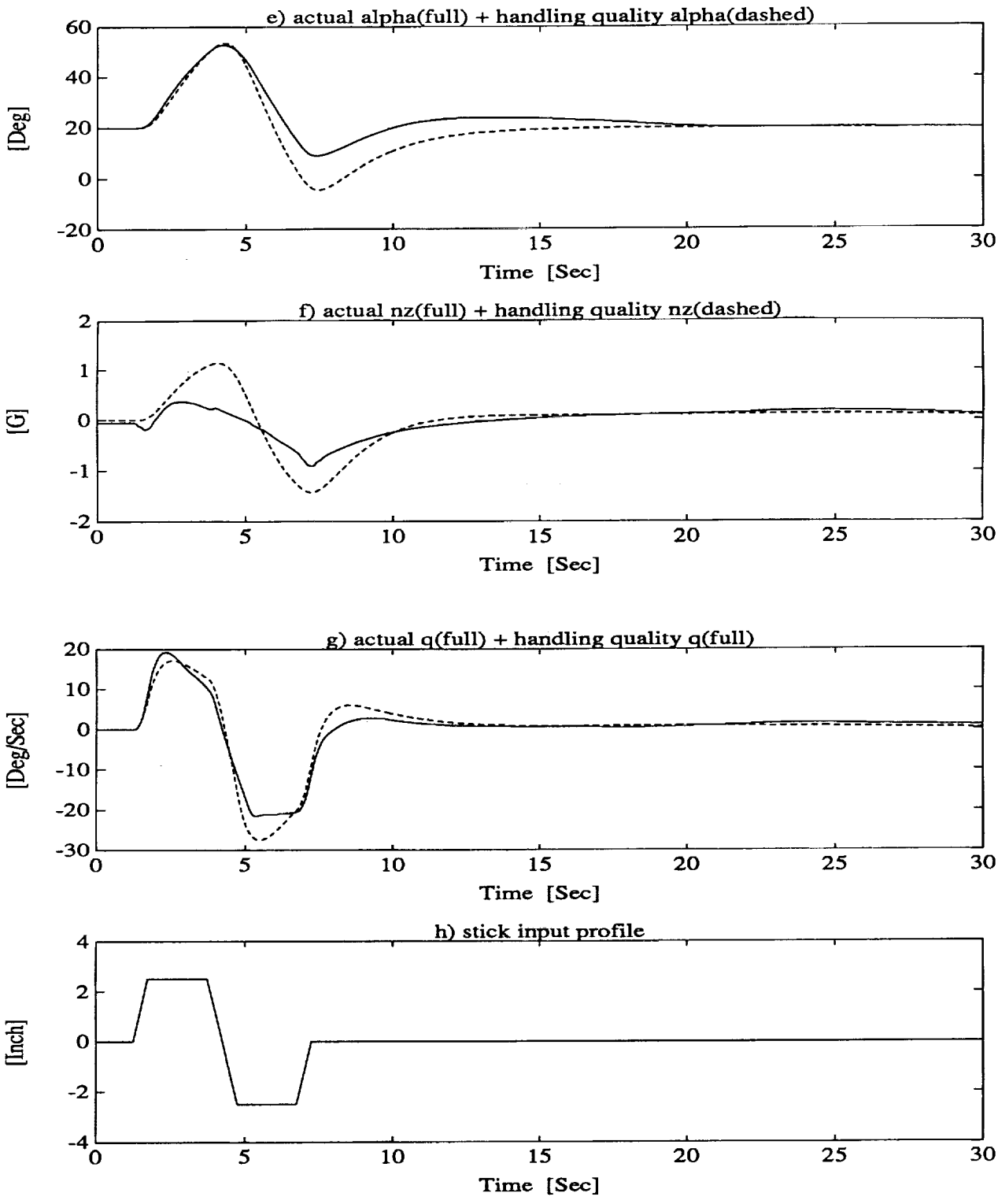

Figure 15: Time response of the nonlinear simulation with μ controller

Before synthesizing the μ controller we synthesized an H_∞ controller that should meet only the performance specifications at $\alpha = 35$ *Deg.* In this section we shall compare our controller (UM) performance with the baseline controller performance in a maneuver that includes a full throttle and a longitudinal stick input as described in Figure 16i. A much higher stick deflection is needed for trimming the aircraft with the baseline controller relative to UM controller. Since the aircraft goes through large excursion in angle of attack and Mach number the nonlinearities in the equations of motion play an important role in these simulation. Also as shown in Figure 16l there is a substantial roll angle during the maneuver, so the lateral dynamics also are important.

Initial the aircraft is in trim at $\alpha = 35$ *Deg*, H = 15000 *ft* and at Mach = 0.205. As can be seen from Figure 16 both controllers are very close to each other.

This example is one of many comparisons we did between our control laws and the baseline control law. Our controllers performed as well as or better then the baseline controller in all cases.

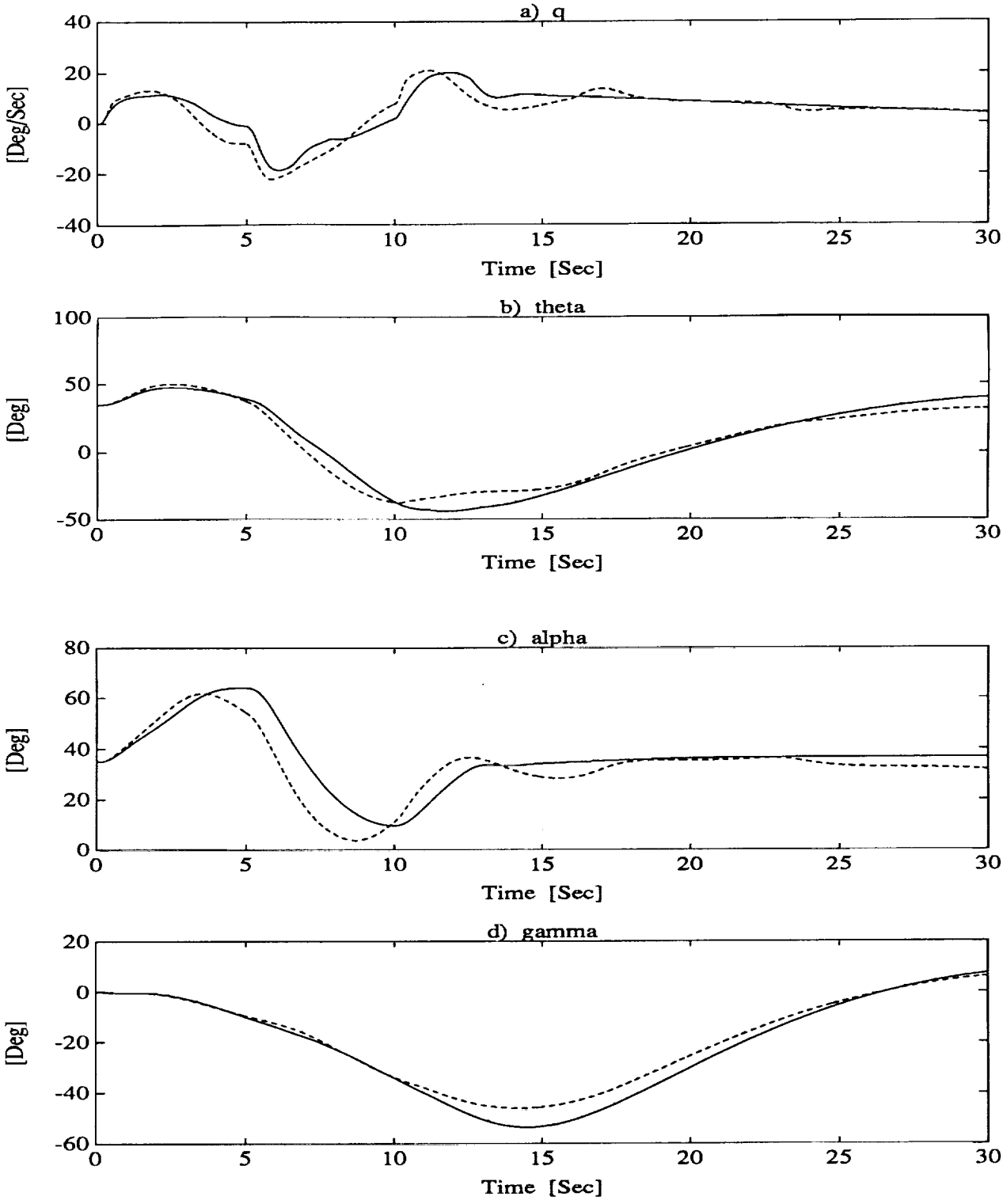

Figure 16: Baseline Controller(full) and UM Controller(dashed)

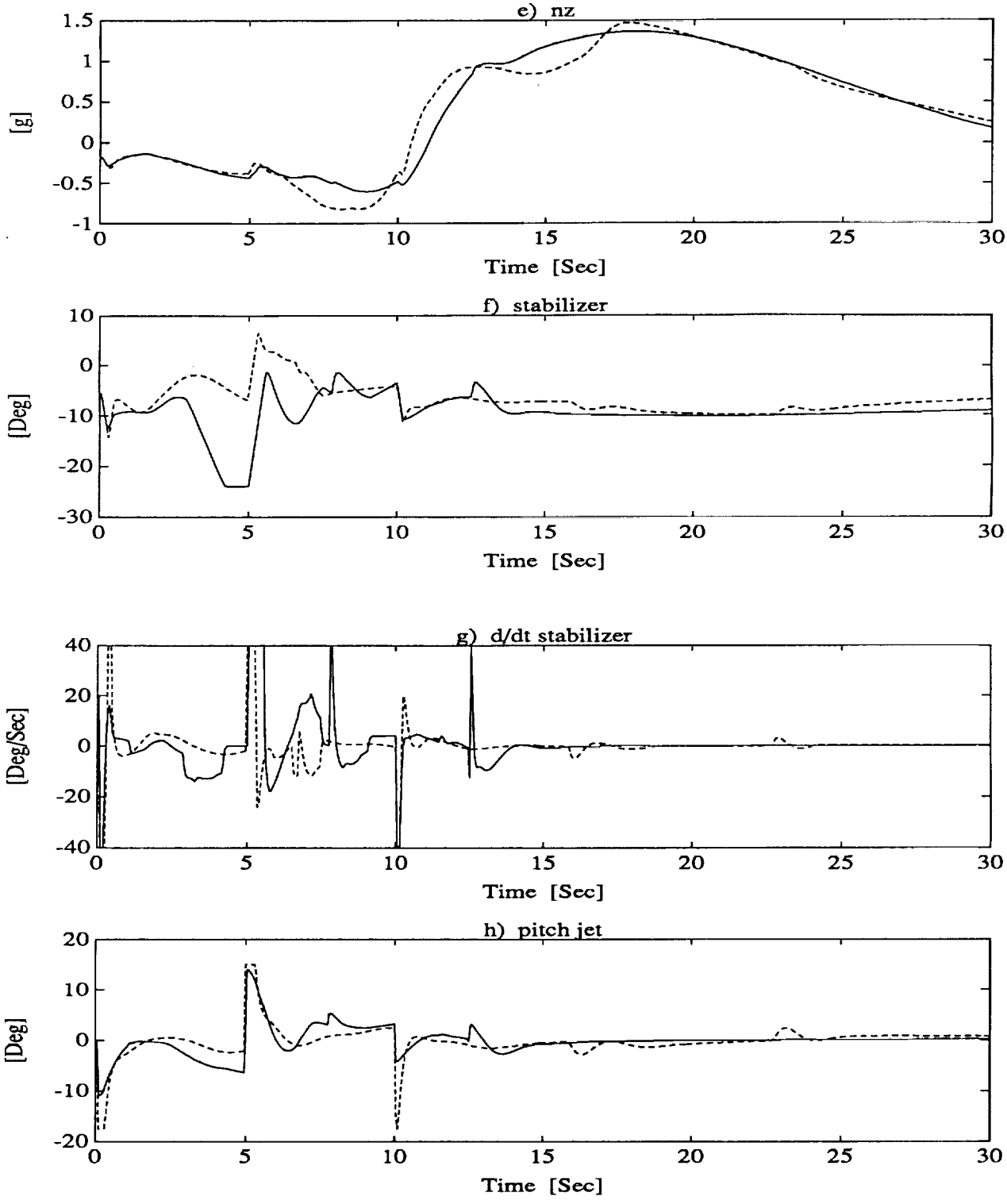

Figure 16: Baseline Controller(full) and UM Controller(dashed)

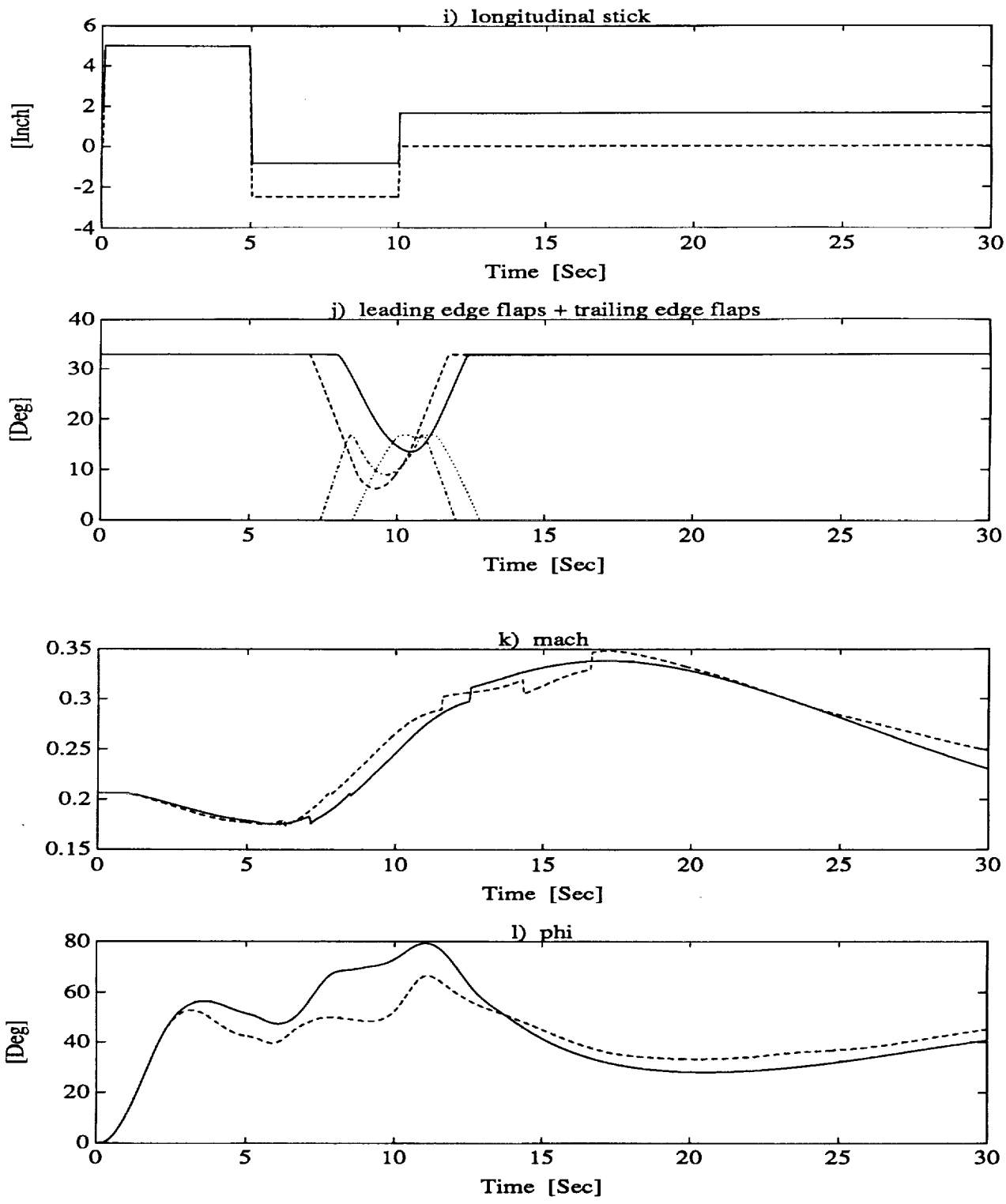

Figure 16: Baseline Controller(full) and UM Controller(dashed)

7 Conclusions and Plans for Further Research

The methodology outlined in this report has wide application to design of H_∞ based control laws for aircraft. Both the H_∞ and μ synthesis control laws provide excellent dynamic response characteristics. Once the basic techniques have been developed control laws can be designed quickly and these control laws provide dynamic response characteristics which are as good or better than those of the baseline control law. The μ synthesis control laws show better performance at off nominal flight conditions than do the H_∞ control laws when evaluated using the linear simulation, but both control laws yield essentially the same response in the nonlinear simulation. Addition work is needed in evaluating the robustness properties of these two control laws. We also need to study the transitioning of the control laws from a pitch rate command to an angle of attack command as angle of attack increases. We are beginning to work on the design of the nonlinear dynamic inversion control law.

References

[1] Military Standard, "*Flying Qualities Of Piloted Aircraft. MIL–STD–1797A*", Mar. 31, 1987.

[2] G.J. Balas, J.C. Doyle, K. Glover, A.K. Packard and R. Smith, "*μ-Tools: The μ-Analysis and Synthesis Toolbox*" , MUSYN Inc. and The Mathworks, April, 1991.

[3] G.J. Balas, J.C. Doyle, A.K. Packard, "*MUSYN Robust Control Short Course – A Collection of Notes and Papers*", September 11–14 1989, Arcadia, California.

[4] G.J. Balas, J.C. Doyle, A.K. Packard, "*MUSYN Robust Multivariable Control Short Course*", August 5–8 1992, Minneapolis, Minnesota.

[5] J.C. Doyle, K. Glover, P.P. Khargonekar and B.A. Francis, "*State Space Solutions to Standard H_2 and H_∞ Control Problems*", IEEE Transactions on Automatic Control, Vol. 34, No. 8, August 1989, pp. 831-847.

[6] B.G. Morton and R.M. McAfoos, "*A μ Test for Robustness Analysis of a Real-Parameter Variation Problem*", Proceedings of The American Control Conference, 1985, pp. 135-138.

[7] B.A. Francis, "*A Course in H_∞ Control Theory*", Springer-Verlag, Berlin, Germany, 1987.

[8] A.W. Naylor and G.R. Sell, "*Linear Operator Theory in Engineering and Science*", Springer-Verlag, New - York, 1982.

[9] J.C. Doyle, J. Wall and G. Stein, "*Performance and Robustness Analysis for Structured Uncertainty*", Proceedings of the 21$^{st.}$ Conf. on Decision and Control, December 1982, pp. 629-636.

[10] J.C Doyle, "*Analysis of Feedback Systems With Structured Uncertainties*", IEE Proceedings, Vol. 129, Part D, No. 6, November 1982, pp. 242-250.

[11] W. Jr. Bihrle, "*A Handling Qualities Theory for Precise Flight Path Control*", AFFDL-TR-65-198, June 1966.

[12] D.J. Moorhouse and W.A. Moran, "*Flying Qualities Design Criteria for Highly Augmented System*", IEEE 1985 National Aerospace and Electronics Conference NAECON, May 1985.

[13] G.C. Krekeler, D.J. Wilson and D.R. Riley, "*High Angle-of-Attack Flying Qualities Criteria*", McDonnell Aircraft Company, MCAIR 89-018, 1989.

[14] A.E. Bryson and Y.C. Ho, "*Applied Optimal Control*", Hemisphere Publishing Corporation, 1975.